Kinetics of UV Photodegradation of DNA Model Systems in a Room Temperature Sugar Glass

A Senior Honors Thesis

Presented in Partial Fulfillment of the Requirements for Graduation with Research Distinction in Chemistry in the undergraduate colleges of The Ohio State University

by

Marc Paul Leslie Coons

The Ohio State University
June 2009

Project Advisor: Professor Bern Kohler, Department of Chemistry

Acknowledgements

I would like to thank my advisor, Professor Bern Kohler, for the opportunity to work on this project starting my second quarter of freshman year. Your confidence and constant support of me during this project is greatly appreciated and without it I would not have gotten as far as I did. I would also like to thank Professor Terry Gustafson for his support not just in research, but for all the advice and conversations we had outside the realm of chemistry.

To Javad Azadi, Nicole Dickson, Jessica Donehue, Kimm de La Harpe, Joe Henrich, Yu Kay Law, Chris Middleton, and Charlene Su: you are a great bunch of people who made working in the basement of Newman and Wolfrom not so painful and lonely. It has been a pleasure to work with you guys and thanks to all of you for the significant amounts of help you have given me in research, on schoolwork, and in general.

A special thanks is deserved by my father, Paul Coons, who has been an extraordinary pillar of strength in my life and has been there to support me since the beginning.

Abstract

DNA undergoes photochemical reactions when exposed to ultraviolet (UV) radiation. The photochemical products cause mutations which can lead to cancer and apoptosis. Upon exposure to UV radiation, the major photochemical products are cyclobutane pyrimidine dimer (CPD) and the pyrimidine-(6-4)-pyrimidone photoadduct. After photoexcitation, relaxation from the excited $^1\pi\pi^*$ state results in a [2 + 2] cycloaddition between adjacent thymine bases forming CPDs. Due to the ultrafast timescale of dimerization, it has been proposed that thymine bases must have the proper geometry before excitation. It is the purpose of this study to obtain experimental evidence for this theory: the ground state control theory. To prepare a system of thymine bases, a room temperature trehalose/sucrose glass was used to encapsulate free thymine bases, thymidine monophosphate (TMP), and thymidylyl-(3'-5')-thymidine (dTpdT) in a pH 7 buffer solution. The glass samples were irradiated with 254 nm UV light from a mercury lamp. A UV-Vis absorption spectrum was recorded for each sample at varying time intervals of irradiation until there was no further decrease in absorbance at 260 nm, indicating that the photochemical reaction is at equilibrium. The quantum yields in the sugar glass increased at least 10-fold for thymine and TMP and over 40-fold for dTpdT relative to the quantum yields in buffered solution.

Contents

List of Figures

List of Tables

Chapter 1
Introduction

Deoxyribose nucleic acid (DNA) is known to undergo photochemical reactions when exposed to ultraviolet (UV) radiation. Upon exposure to UV radiation, the major photochemical products that form are cyclobutane pyrimidine dimers (CPD) and the pyrimidine-(6-4)-pyrimidone photoadduct.[1] These photoproducts result in structural changes of the DNA, which can lead to a variety of negative effects in the cell including mutations resulting from mistranscriptions of genomic sequence, replication of sequence error to future daughter cells, carcinogenesis, and programmed cellular death through apoptosis.[2-4] The formation of CPDs results when a thymine base is photoexcited with an ultraviolet photon and has an adjacent thymine base with which to react. It is our hypothesis that these thymine bases must have the proper geometric configuration for photoexcitation to successfully result in a CPD, and controlling the geometry of the thymine bases should affect the quantum yield of their photodegradation.

The thymine systems of interest for this study are free thymine bases, thymidine monophosphate (TMP), and thymidylyl-(3'-5')-thymidine (dTpdT). These model systems provide only thymine bases with a known number of bases per system (i.e. free thymine bases are just the base itself while TMP is a nucleotide with a single thymine base, and dTpdT is a nucleoside with two bases), which allows for well-controlled experiments as opposed to using long, non-uniform chains of single-stranded DNA.

1.1 Objectives of this Study

The purpose of the experiments conducted in this study is to obtain a better understanding of environmental effects on the quantum yield of photodimerization for various thymine model systems. Using a germicidal lamp as a source of UV light, the encapsulated samples were irradiated at various time intervals. By quantitatively studying the change in absorbance at λ_{max}, which is the wavelength of maximum absorption for the chromophore of interest, it will be possible to determine the quantum yield of photodegradation for the DNA model systems. Then, by using circular dichroism (CD), it will be possible to detect any changes in the geometrical conformation of the model systems upon encapsulation in the sugar glass.

After an introduction about the discovery and history of nucleic acids, there will be a brief review of relevant literature. Then a description of the theories and procedures behind the experimental techniques will be given with a full analysis of the data and its interpretations. The two main themes of this thesis are the determination of the quantum yield for the DNA model systems in solution and in sugar glass and the qualitative study of the structural changes encountered by the model systems when encapsulated using CD.

1.2 The DNA Model and its Components

To fully analyze and interpret the experimental results of this study, a brief review of nucleic acid chemistry, photochemistry, and photophysics will be given. This review will start with a history of nucleic acid discovery and conclude with the current model of DNA as made from decades of experiments. Other topics in this section will include nomenclature, electronic excitation of molecules, and the mechanism of thymine dimerization.

1.2.1 Discovery of Nucleic Acids

Though it was unknown to scientists at the time, deoxyribonucleic acid (DNA) was discovered in 1869 by Friedrich Miescher who was a researcher in physiological chemist Felix Hoppe-Seyler's laboratory.[5] Miescher obtained his samples of DNA from the white blood cells isolated from pus on used surgical bandages by adding hydrochloric acid to precipitate a gelatinous material containing carbon, hydrogen, nitrogen, oxygen, and phosphorus.[6] Soon after Miescher obtained samples of DNA from white blood cells, Hoppe-Seyler obtained a similar substance from yeast cells that was later on determined to be ribonucleic acid (RNA).[5] In 1889, Albrech Kossel discovered the four bases in DNA (cytosine, guanine, adenine, and thymine) and was subsequently awarded the Nobel Prize in Physiology or Medicine in 1910.[7] Then, in 1891 Kossel also discovered that the majority of carbon coming from gelatinous precipitate found by Miescher was due to a sugar that was later identified as ribose (RNA) and deoxyribose (DNA).[8] Figure 1.1 on the next page illustrates the structures of the four bases in DNA and uracil, which takes the place of thymine in RNA, as well as the other building blocks of DNA and RNA. In 1919 Phoebus Levene proposed the structure of DNA: short chains of nucleotide units bound together by phosphate groups in a very fixed order.[9] However, in 1937 William Astbury produced the first X-ray diffraction pattern of DNA, which showed that it was a very long chain with a regular structure, but not necessarily with a fixed order of nucleic acids.[10] It was not until 1963 when James D. Watson and Francis Crick made their famous proposal in Nature about the structure of DNA, which has come to be the accepted model for double stranded DNA.[11]

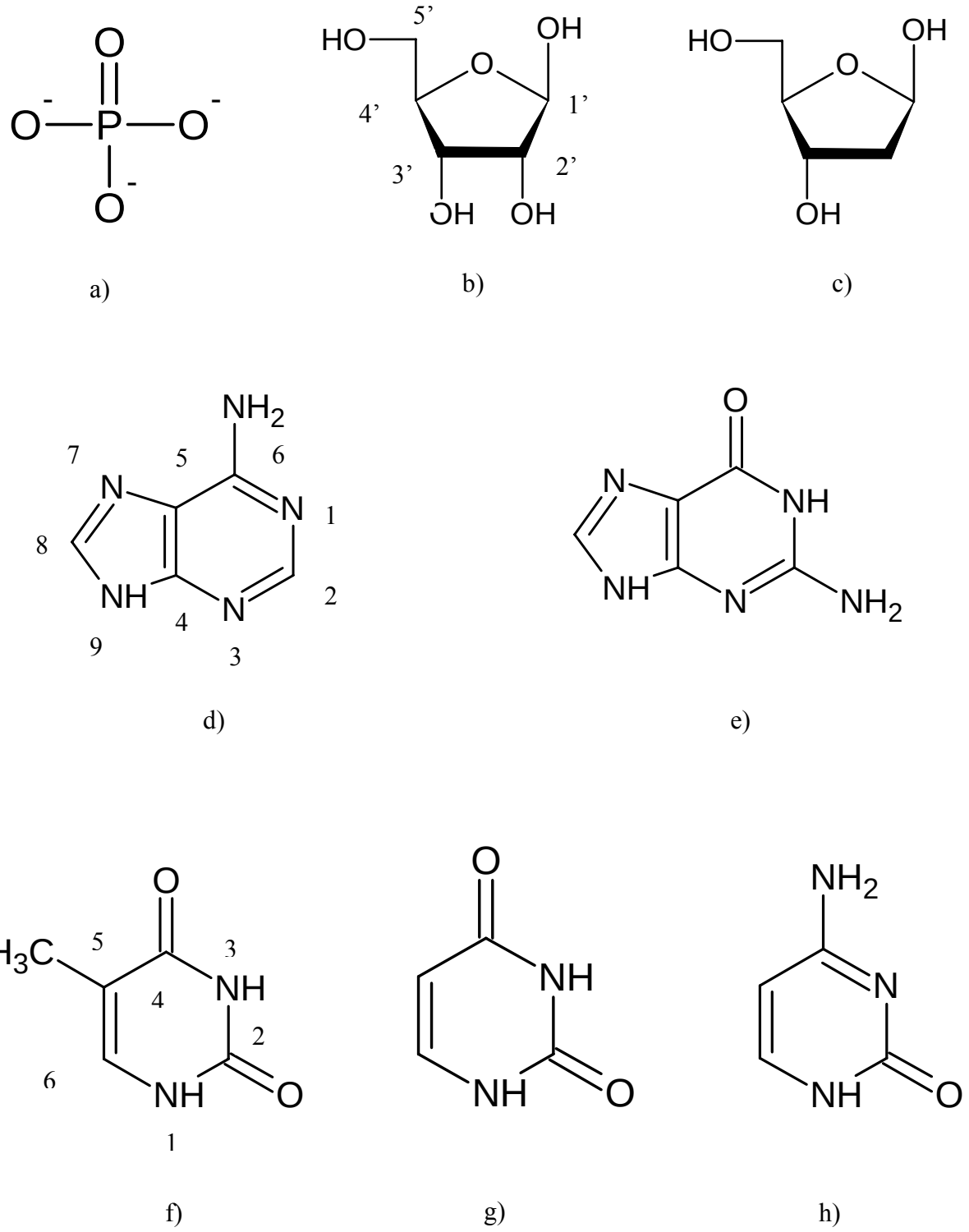

Figure 1.1: The structures of the components of DNA and RNA: a) phosphate, b) D-ribofuranose, c) 2'-deoxy-D-ribofuranose, d) adenine, e) guanine, f) thymine, g) uracil, and h) cytosine

1.2.2 Properties of Nucleic Acids

As can be seen from Figure 1.1, the bases that make up nucleic acids are flat molecules because all of the atoms are sp^2 hybridized and lie in the same plane. The pyrimidines are thymine, uracil, and cytosine and are six-membered rings. The purines are adenine and guanine and are bicylic rings consisting of a six-membered ring fused to a three-membered ring. In all cases, the bases are heterocyclic rings because of the nitrogen atoms that compose portions of the ring as opposed to being completely made from carbon atoms. The pyrimidine and purine rings are aromatic which allows for delocalization of electrons in molecular orbitals. The aromaticity of the rings allows for electron transitions to take place between a π-orbital of the ground state to a vacant, excited state π*-orbital. This type of transition generally occurs in the Ultraviolet-Visible (UV-Vis) spectrum and will be discussed in more detail in Section 1.3.

The bases from Figure 1.1 that make up the seemingly limitless possible combinations of DNA and RNA sequences exhibit many unique and interesting properties that allow them to encode our genome. In order for two single strands of DNA to become double stranded DNA, called a duplex, there has to be significant interactions between nucleic acid bases on opposing strands. This interaction was proposed by Watson and Crick and has therefore been termed Watson-Crick base pairing. Base pairing occurs when a purine such as adenine (A) or guanine (G) forms hydrogen bonds with a pyrimidine, such as thymine (T) or cytosine (C). The normal Watson-Crick base pairs are between adenine and thymine, which forms two hydrogen bonds, and between guanine and cytosine, which forms three hydrogen bonds. The extra hydrogen bond that forms between a G·C pair makes this base pair harder to break compared to an A·T base pair. However, there are many instances of non-Watson-Crick base pairing such as A·C and G·T base pairs, pyrimidine-pyrimidine and purine-purine base pairs, and other combinations.[12]

When Watson and Crick tried to study the phenomenon of base pairing further, they discovered that nucleic acid bases tended to stack with themselves rather than form base pairs, even after putting 1:1 ratios of adenine and thymine or guanine and cytosine in solution.[12] They discovered that the bases preferred to aggregate and form columns of two to three bases. Depending on the solvent, the number of bases that stacked together in these columns was controlled by altering the intermolecular interactions between the solvent and the bases, the solvent and the base pairs, and between solvent molecules.[12] It was shown that the free energy of base stacking for uridine, thymidine, and cytidine were all slightly positive numbers, and therefore they are all endergonic processes. However, the entropy of base stacking found in these monomers was negative, and therefore it was an entropically disfavored process. Base stacking tends to be more favorable in single stranded and duplex DNA, but varies depending on the base sequence.[12]

1.2.3 The Current Understanding of DNA

When the purines and pyrimidines become attached to the carbons at the 1' position of the sugars from Figure 1.1, they form a unit called a nucleoside. When these nucleosides become attached to a phosphate group at the 5' position of the sugar, they form a nucleotide. An example of a nucleoside and nucleotide unit of a DNA molecule is shown on the next page in Figure 1.2. The base, sugar, and phosphate nucleotide unit is the building block of DNA and RNA molecules. The two major differences between DNA and RNA molecules are that in DNA, the sugar attached to the DNA base has no hydroxyl group at the 2' carbon position as shown in Figure 1.1 and that the RNA base uracil does not show up in DNA strands. Likewise, thymine does not show up in RNA molecules.

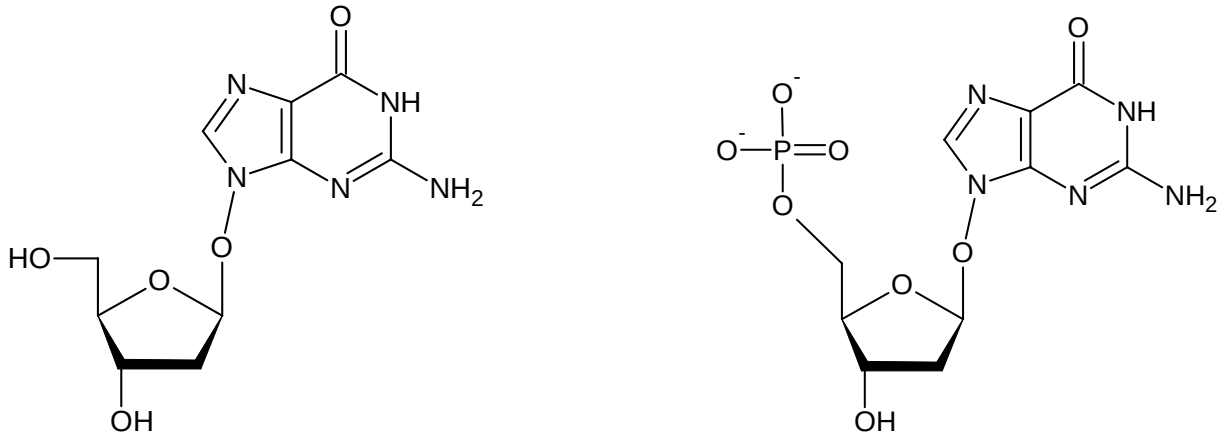

Figure 1.2: Structures of a) nucleoside and b) nucleotide with a guanine base.

Nucleotide units such as the one shown in Figure 1.2 are used to build incredibly long chains of DNA molecules. Two nucleotides bond to each other through a 3'-5' phosphodiester linkage. A phosphodiester linkage is formed between an oxygen atom on the phosphate group attached to the 5' carbon of one nucleotide and the 3' carbon of the other nucleotide. This process results in the release of a water molecule through a condensation mechanism. By convention, DNA is labeled as having a 3' end and a 5' end. The 3' end is the "bottom" of the DNA molecule and is the only location where a 2'-deoxy-D-ribofuranose sugar has a free hydroxyl group. The 5' end is considered the "top" of the DNA molecule and is the only location of the molecule where there is a free phosphate group attached to the 5' carbon of the 2'-deoxy-D-ribofuranose sugar. When many nucleotides come together, they form a single strand of DNA. With the help of certain enzymes to facilitate the process, two single strands of DNA come together to form a DNA duplex, usually with the expected Watson-Crick base pairs. It is important to note that the geometry of Watson-Crick base pairs is such that it allows for any sequence of base pairs while still maintaining a uniform helix shape without any distortion.[12] Figure 1.3 below shows duplex

DNA in B-form, which is just one particular orientation of the backbone and base pairs that can occur.[13]

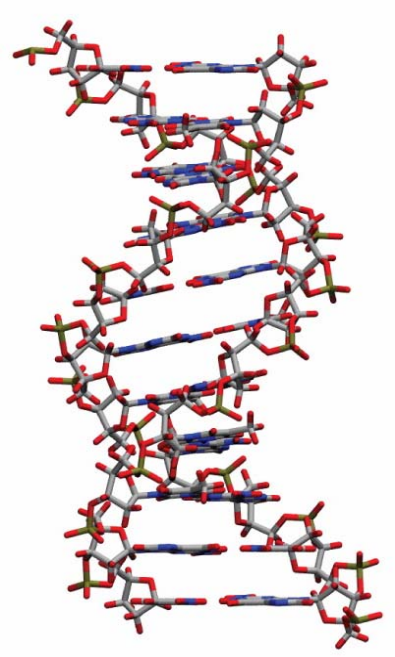

Figure 1.3: Structure of B-form DNA

As can be seen from Figure 1.3 above, when two single strands of DNA come together to form a duplex, the amount of base stacking that occurs increases as the result of a helix formed from the base pair interactions holding the strands together. The two single strands that make up a DNA duplex run antiparallel, which means one strand goes in the 3' to 5' direction and the complementary strand runs in the 5' to 3' direction relative to each other. There are two other known forms of DNA not shown in Figure 1.3: A-form and Z-form DNA. Only B-form and Z-form DNA have been found in living cells, however.[14] The conformation of DNA depends on factors such as hydration level, base pair sequence, the amount and orientation of supercoiling, the nature of the solvent and environment, and the concentration and type of metal found in the solution.[15]

1.3 Electronic Excitation Processes

When a photon of the proper energy is absorbed by a molecule, an electron is excited to a higher electronic energy level. Generally, this requires a photon with a wavelength in the UV-Vis range. Upon absorption and excitation to a higher energy level, the electron has several different pathways it can take to return to the ground state, labeled here as S_0. Figure 1.4 below shows a Jablonski Diagram, which is a simplified schematic of the possible processes the electron can undergo.

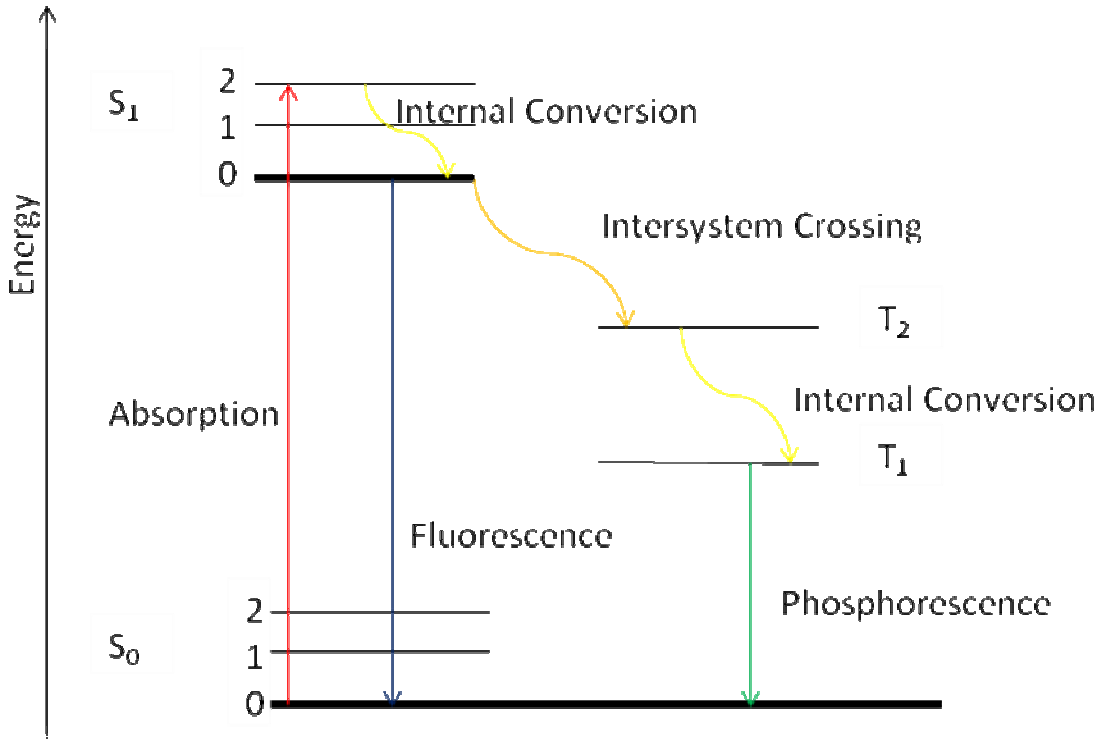

Figure 1.4: A Jablonski Diagram showing the possible fates of an electron excited from the ground state, S_0, to an excited S_1 state.

The red line indicates absorption in which an electron is excited to a higher electronic energy level, labeled here as S_1. The thinner lines shown between each electronic state represent vibrational energy levels, which are less energetic and are closer together. Absorption of a photon can lead to an excitation to a higher electronic, vibrational, and rotational energy state,

but the latter type is not shown in this diagram for simplicity. The process of internal conversion, shown as the wavy yellow arrows, is the relaxation of an electron to a lower vibrational energy level without the release of a photon. To conserve energy, the excess energy is dissipated through nonradiative processes such as the transfer of excess energy to another molecule. The blue arrow shows the process of fluorescence, which occurs when a photon in an excited electronic state relaxes to another electronic state, shown here as S_0, with the release of a photon having a wavelength corresponding the energy difference between the two states (see Equation 2.2).

However, there is another pathway that electrons can take instead of fluorescence. The orange wavy arrow represents intersystem crossing that occurs when an electron relaxes from an excited electronic state to a lower energy triplet state, shown here as T_2. The process of intersystem crossing is nonradiative and the excess energy is dissipated in similar methods as in internal conversion. Once in the triplet T_2 state, internal conversion can occur bringing the electron to a lower T_1 energy state. Relaxation from a triplet state back to the ground state is done through the process of phosphorescence. This process results in the release of a photon with an energy corresponding to the energy difference between the T_1 and S_0 state.

The lifetime of an electron that fluoresces to the ground state is significantly faster than the lifetime observed if it phosphoresced. A typical lifetime of fluorescence is less than 10 nanoseconds, while that of phosphorescence is typically greater than 1 millisecond. When an electron phosphoresces, it must undergo a "forbidden" transition, while an electron that fluoresces does not. A triplet state is one in which the electron started with a singlet spin multiplicity, but after intersystem crossing went to a higher spin multiplicity. An electron can obtain two types of spins: up and down. When an electron undergoes intersystem crossing, it

switches from spin up to spin down or vice versa. The transition is considered to be forbidden because it violates the Pauli Exclusion Principle which says that no two fermions (i.e. an electron or particles with non-integer spin) can occupy the same quantum state simultaneously. Therefore because the electron flipped its spin from what it originally was in the ground state, it cannot easily return to the ground state, which explains the longer lifetime observed for a triplet state.

1.4 Review of Related Research

1.4.1 Photochemistry and Photophysics of Thymine Dimerization

The discovery that DNA undergoes photochemical reactions when exposed to ultraviolet radiation led researchers to pursue investigations about the mechanisms behind these reactions and the photoproducts they were forming. When it was shown that thymine dimers cause effects such as immune suppression and mutations that lead to carcinogenesis and apoptosis, significant amounts of research aimed at investigating the mechanism of dimer formation began. It has been proposed that the mechanism for the formation of the dimer occurs through a [2 + 2] cycloaddition reaction. For this to occur, an ultraviolet photon excites electrons from the π bond between carbon 5 (C5) and carbon 6 (C6) of a thymine molecule. If the excited thymine molecule is adjacent to another thymine molecule and they are aligned properly at the moment of photoexcitation, then a thymine dimer can form. Figure 1.5 on the next page shows the fate of a thymine molecule upon excitation from an ultraviolet photon.

When a system of thymine molecules absorbs a UV photon, it is the $^1\pi\pi^*$ state that is most heavily populated.[13] Because the oscillator strength of this transition is so great, it is called a bright state. It was shown that 60 % of the population of a $^1\pi\pi^*$ state returns to the ground

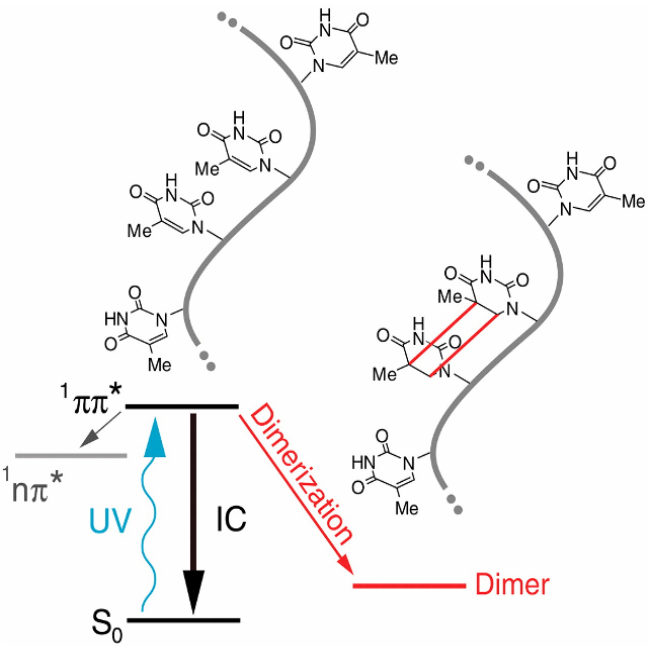

Figure 1.5: Energy level diagram showing the fate of an excited thymine base (Adapted from a figure in Reference 16).

state via nonradiative internal conversion processes regardless of the solvent chosen.[17] It has also been shown that emission from the $^1\pi\pi^*$ state is an ultrafast process that happens a femtosecond timescale.[18] However, there are other pathways excited electrons can take rather than internal conversion or relaxation to form a dimer with an adjacent thymine. It has been shown that all nucleobases can be promoted to dark states that have very low oscillator strength.[18] These dark states include the $^1n\pi^*$ state, the $^3\pi\pi^*$ state and the $^3n\pi^*$ states. Formation of the $^3\pi\pi^*$ state occurs due to intersystem crossing from a $^1n\pi^*$ state that has excess vibrational energy.[13,18]

Due to the ultrafast process of relaxation from the $^1\pi\pi^*$ state, dimer formation occurring between thymine molecules will be observed primarily in multimers of single and double stranded DNA. Since there are only femtoseconds to photoreact with an adjacent thymine molecule, the thymine molecules must already be aligned properly and sufficiently close

together. However, for bases that exist as monomers, there is no adjacent thymine molecule bonded to a backbone. Therefore, the monomers need to form dimers through another, longer lived pathway. Since relaxation from a triplet state has a larger lifetime, it is proposed that the main pathway for dimer formation in monomers is due to relaxation from $^3\pi\pi^*$ states.

1.4.2 Solvent and Environmental Effects on Dimerization Yields

Computational studies have examined the effects of various types and amounts of solvents on the quantum yield of photodegradation. It was shown that the quantum yield of photodegradation decreased when solutions of 40 % and 60 % ethanol by volume were used to dissolve dTpdT molecules.[19] Similar results were seen when solutions of 50 % dioxane by volume was used. It was suggested that the co-solvents were affecting the conformation of the dTpdT molecules and therefore fewer molecules were sampling the proper conformation for dimerization to occur and therefore the quantum yield of photodegradation was lowered. The computational study also showed that there are ideal conformers that a dTpdT molecule must obtain in order to form a dimer.[19]

Studies done on the quantum yield of photodegradation in frozen solution and dried films have also suggested that dimerization is structure dependent. It was observed that when solutions of thymine bases were irradiated, only a small portion were able to form dimers. When the solutions were frozen and irradiated a second time, more dimers were able to form.[20] This observation suggests that the crystalline structure of water formed upon freezing could be forming aggregations of thymine monomers. The aggregations allow for thymine monomers to more readily find each other. The frozen water crystals could also be affecting the conformation of thymine multimers by restricting free rotation of thymine molecules with respect to the sugars

to which they are attached. Similar results were seen in thin films made from metal alkoxide compounds.[21]

1.5 Hypothesis

The hypothesis of this study is that thymine dimerization is structure dependent and that by changing its environment, the yield of dimers will be altered. By performing irradiation experiments in a room temperature sugar glass that will be used to encapsulate three thymine systems (thymine bases, TMP, and dTpdT), it is expected that there will be an increase in the quantum yield of photodegradation for dTpdT, but not the monomers. It is believed that this sugar glass will create a restrictive environment around the dTpdT molecules and prohibit them from having complete rotational freedom as they would in solution, and therefore a larger fraction of these molecules will be trapped in geometries very close to the ones need for dimerization. More dTpdT will then be able to photoreact to form thymine dimers. However, for the two monomers of thymine being used in this study, there should only be a modest, if any at all, increase in the quantum yield of photodegradation because the sugar glass will be unable to affect the conformation of these monomers.

Chapter 2

Theory of Experimental Methods

2.1 Absorption Spectroscopy

The interaction of light with matter provides the foundation for all of the spectroscopic techniques used in this study. The two main techniques used to study the photochemical reactions of these experiments were UV-Visible molecular absorption spectroscopy and circular dichroism (CD). In molecular absorption spectroscopy, a series of varying wavelengths is passed through a sample of interest and a reference cell containing only the solvent. The amount of transmission, which can be related to absorption, for the sample is determined by measuring how much light hits the detector relative to the reference. Absorption occurs when a photon corresponding to the proper energy interacts with the sample to excite an electron from its ground state to a higher excited state (see Figure 1.4 and its discussion). CD spectroscopy works on the same principle as molecular absorption spectroscopy in that a selected series of wavelengths is used to excite the molecules in the sample. However, in CD the radiation is modified so that light interacting with the sample is both left-circularly and right-circularly polarized. The difference in absorption of the left and right-circularly polarized light is measured by the CD instrument. The measurement of CD provides information about the ellipticity, which can be related to structural features, for a given molecule.

2.2 Properties of Light

Before discussing the theory behind the experimental techniques used in study, it is first important to discuss the basic properties of light since it is the most important source for the instrumentation. As light, which is a form of electromagnetic radiation, propagates through space, it consists of an electric field vector **E** and a magnetic field vector **B** which is orthogonal to **E**. Figure 2.1 below shows this pictorially.

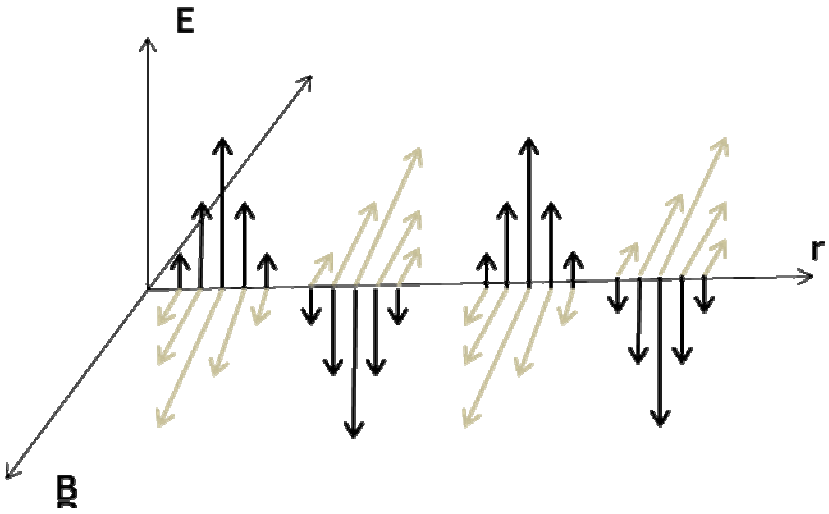

Figure 2.1: Pictorial representation of the components of electromagnetic radiation; black arrows represent the electric field **E** and gray arrows represent the magnetic field **B**.

E is free to rotate around its line of propagation, shown as the vector **r** above, in a sinusoidal oscillation. It is these sinusoidal oscillations in time that give rise to the wave nature of light. In another type of spectroscopy called linear dichroism, the propagation of **E** is restricted such that it remains on a single plane with respect to **r**. In the spectroscopic techniques used in this study, it is only the electric field that is considered in the measurements made and will be the center of the rest of this discussion. In UV-Vis spectroscopy, the radiation source is not polarized in any particular way as it is for CD. The radiation used for CD is changed into left and right-circularly

polarized light via a photoelastic modulator. Figure 2.2 below shows the electric field of left and right-circularly polarized light.

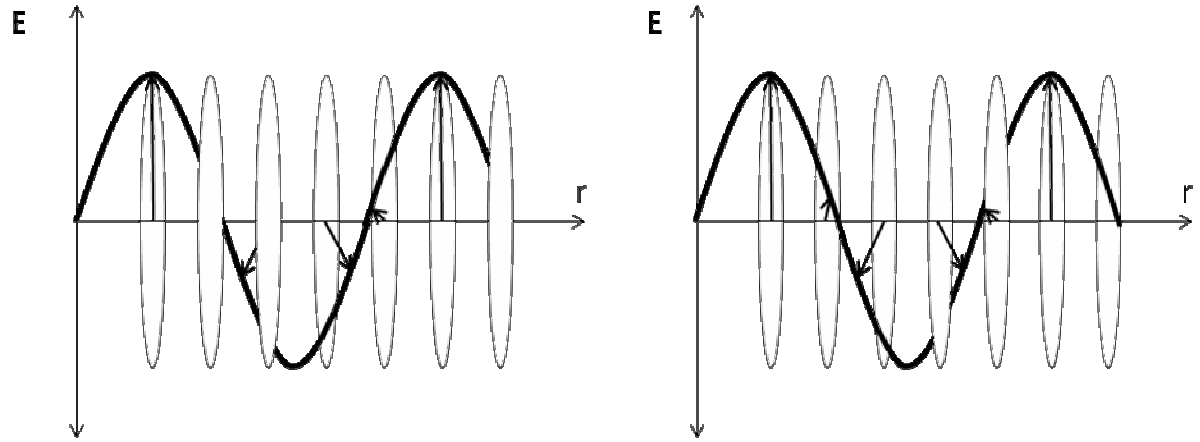

a) b)

Figure 2.2: Circularly polarized light; a) left-circularly, b) right-circularly

The left and right components of **E**, written as $\mathbf{E}_l$ and $\mathbf{E}_r$, are vector quantities that oscillate in different directions with respect to each other but at equal velocities since they are still forms of electromagnetic radiation.[22]

It has been shown that light exhibits both wave and particle properties. It was also discovered that any type of electromagnetic radiation travels through a vacuum with a constant velocity of 299,792,458 m s^{-1}. Since electromagnetic radiation has wave-like properties and a constant velocity, the wavelength λ of such a wave multiplied by its frequency υ must be equal to its velocity c shown in Equation 2.1

$$c = \lambda \upsilon \tag{2.1}$$

Max Planck's work with blackbody radiation led him to discover the relationship between the wavelength or frequency of a photon and its corresponding energy. The higher the frequency

and smaller the wavelength, the more energetic the photon is as seen from the following equations

$$E = h\upsilon = \frac{hc}{\lambda} \tag{2.2}$$

In 1924 Louis de Broglie proposed the wave-particle duality of electromagnetic radiation by relating the momentum of a particle to a particular wavelength in the famous equation

$$p = \frac{h}{\lambda} \tag{2.3}$$

Despite the many seemingly counterintuitive discoveries about light, the field of quantum mechanics has changed the way electromagnetic radiation is viewed and has opened the doorway for many incredibly powerful techniques used to study chemical phenomenon.

2.3 Spectroscopy

All of the experiments performed in this study take advantage of some form of spectroscopy. This section will describe the physics of molecular absorption and CD spectroscopy as well as actinometry in order to more fully understand the methods and results of the experiments.

2.3.1 Molecular Absorption

In molecular absorption spectroscopies such as UV-Vis and CD, a radiation source is used to promote electrons to an excited electronic level. However, not all of the radiation is absorbed or used by the molecule for this excitation. Some of the incident light is passed through the sample and is able to reach the detector at the end of the instrument. Consider Figure 2.3 below, which shows some of the ways the intensity of the original radiation source, I_0, can be diminished.

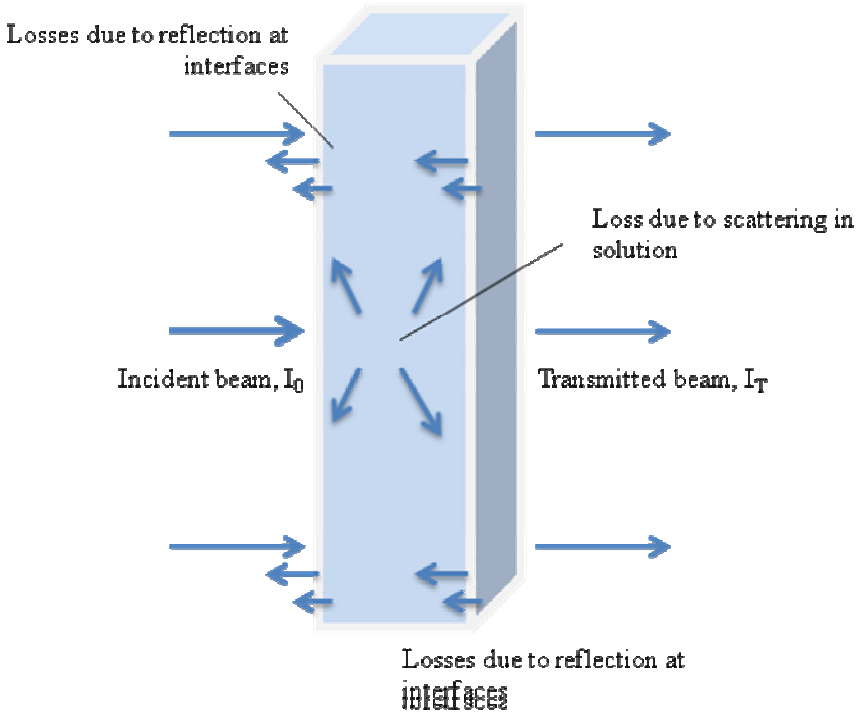

Figure 2.3: Reflection and scattering processes that occur when a cuvette is irradiated.

Apart from molecules of the sample absorbing radiation, there is loss of intensity due to reflection at the air-glass, glass-solution, and solution-glass interfaces of the cuvette and scattering from the solution. For radiation that interacts with the sample, there are three consequences that result. The first consequence is stimulated absorption which occurs when an applied field from the radiation source causes an electron to be promoted to a higher energy level. Stimulated absorption will cause a decrease in the intensity of the original radiation source I_0. The second consequence is stimulated emission which occurs when the same field applied to the sample forces an excited electron to return to the ground state resulting in the emission of a photon. Stimulated emission results in a photon that is co-linear with and has the same phase as the applied field. Therefore this type of emission will not result in a gain nor loss of intensity from I_0 as stimulated absorption will. The final consequence is spontaneous emission due to

fluorescence and phosphorescence. Photons emitted from this pathway are random in direction and phase and will therefore also contribute to loss of intensity of I_0.

To make a measurement of absorption, a series of wavelengths are chosen that have sufficient energy for an electronic transition. The ratio of the intensity of the radiation after passing through the sample (I_T) with that of the original (I_0) provides the transmission T as shown below[23]

$$T = \frac{I_T}{I_0} \tag{2.4}$$

The absorbance A of the sample is related to the transmission through the following equation.

$$A = -\log T = -\log \frac{I_T}{I_0} = \log \frac{I_0}{I_T} \tag{2.5}$$

The ratio of I_T to I_0 is measured by preparing a reference cell of the solvent and a sample cell containing the solvent and the molecules of interest and irradiating both with the same wavelengths and light source intensity. Detectors measure the intensity of each beam and compute the ratio for a given wavelength. The calculated ratio corrects for the loss of intensity due to reflection from the interfaces of the cuvette and the solvent. The process of generating an absorption spectrum is shown below in Figure 2.4.

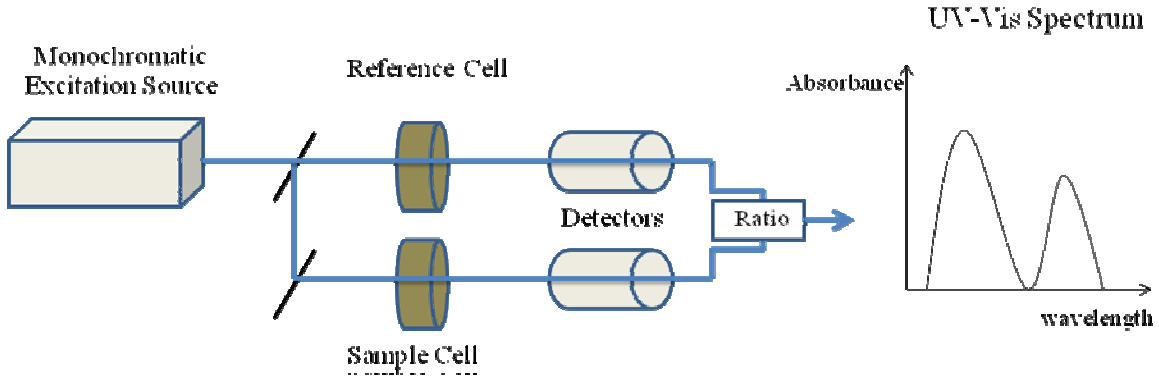

Figure 2.4: Schematic of a UV-Visible spectrophotometer.

The signal of an absorption spectrum is related to the amount of sample being irradiated. Beer's Law is derived by considering a cross sectional area (S) of the sample cell and assuming that any photon that reaches an absorber in this area will result in the capture of a photon. The total area of the capture surfaces within the cross section S is termed dS and the ratio of dS/S is the ratio of the capture surface to the total surface area. This ratio represents the probability of the capture of a photon in the cross section of S. The intensity of the beam entering this cross section, say I_s, is proportional to the number of photons per unit area within S, and the term dI_s represents the intensity absorbed in this same area. The ratio of dI_s/I_s is the fraction of intensity absorbed and is equivalent to the probability of photon capture dS/S. The following relationship is then true where the minus sign is added to present a loss of intensity:

$$-\frac{dI_s}{I_s} = \frac{dS}{S} \tag{2.6}$$

It can be shown that the above equation, after integration and collecting constants, results in the well known version of Beer's Law:

$$A = \log\frac{I_0}{I_T} = \varepsilon\, l\, c \tag{2.7}$$

Here l is the path length of the sample cell, c is the molar concentration, and ε is the molar absorbtivity, which is related to the cross section of the sample molecules and the probability that a photon incident on the molecule will cause an electronic transition. Since absorbance is unitless and the conventional unit of l is cm and c is M, the units of ε must be $cm^{-1}\ M^{-1}$. It is also important to note that the molar absorbtivity is wavelength dependent, and therefore absorbance is too due to the direct relationship between the two.

Despite electronic energy levels being quantized at discrete values, the spectra of molecular absorption experiments generally do not result in narrow peaks at a given wavelength.

Instead they are broadened and extend over a range of wavelengths that is described by one form of the uncertainty principle

$$\Delta E \, \Delta t \geq \frac{\hbar}{2} \tag{2.8}$$

The product of the uncertainty in energy, ΔE, and the uncertainty in the lifetime of the excited state, Δt, cannot be smaller than a specific constant. Other factors that lead to broadening include interactions between sample molecules with each other and the solvent and vibrational and rotational transitions occurring simultaneously.

2.3.2 Circular Dichroism

The technique of circular dichroism relies on the principles of molecular absorption as described in the previous section. However, in circular dichroism the radiation source is modified such that the light becomes left and right-circularly polarized by using a photoelastic modulator. Figure 2.5 below shows the general schematic of a CD instrument.

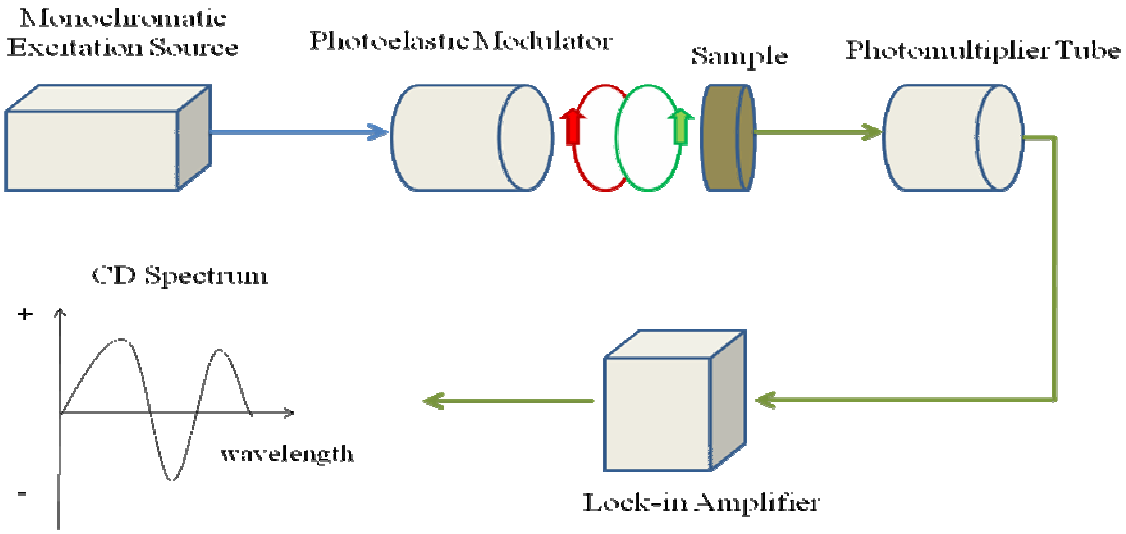

Figure 2.5: Schematic of a circular dichroism instrument.

Circular dichroism is only effective for chiral molecules. The lack of a mirror plane in a chiral molecule means that the electrons of the molecule will also lack a mirror plane.[24] The electrons will then trace out a helix path as they move and will interact with the helices of left and right-polarized light differently.[24] A spectropolarimeter, such as the one used in these experiments, provides a measurement of these different interactions in terms of the ellipticity θ with units of millidegrees. The tangent of the ellipticity is related to the electric field vectors of the left and right-circularly polarized by the following equation:

$$\tan\theta = \frac{E_r - E_l}{E_r + E_l} \tag{2.9}$$

A more useful quantity to show for a circular dichroism spectrum is Δε, which can be related to θ through a series of equations shown below[24]

$$\Delta A = A_l - A_r \tag{2.10}$$

$$\Delta A = l\,c\,(\varepsilon_l - \varepsilon_r) \tag{2.11}$$

$$\Delta\varepsilon = \frac{\Delta A}{l\,c} \tag{2.12}$$

$$\Delta\varepsilon = \frac{4\pi\theta(degrees)}{180\ln 10\ l\,c} \tag{2.13}$$

$$\Delta\varepsilon = \frac{\theta(millidegrees)}{32{,}982\ l\,c} \tag{2.14}$$

Here *l* and c represent the path length of the sample cell and the initial concentration determined before a CD experiment, respectively. As seen by the definition of Δε, it can obtain positive and negative values depending on the extent to which each polarized light interacts with the sample. The manner in which the helical motions of the electrons interacting with the helices of the polarized lights relate to the arrangement of atoms and bonds in space is very complicated and is beyond the scope of this thesis. However, due to the natural chiralty of many biological

macromolecules such as proteins and nucleic acids, CD has become very useful in examining the structure of these molecules or conformational changes during a reaction.

2.3.3 Actinometry

There have been some minor discrepancies in the literature between the methods used for actinometry to determine the photon flux of an irradiation source. Since it is paramount to the success of the kinetics experiments that this be done properly and treated mathematically correct, a first principles derivation was done. The goal of actinometry is to determine the value of I_0 (see Figure 2.3) in order to calculate the number of photons absorbed in irradiation experiments and then ultimately the quantum yield of the system of interest. I_0 is defined as the number of photons incident per area unit per unit of time shown mathematically below

$$I_0 = \frac{photons}{time\ surface\ area} \tag{2.15}$$

The quantum yield is defined using the conventional definition: number of photons causing a photochemical reaction divided by the total number of photons absorbed by the system. The value I_a, which represents the intensity of light absorbed, is related to I_0 through Beer's Law as shown below where A_t is the absorbance at time *t*

$$I_a = I_0 - I_T \tag{2.16}$$

$$I_T = I_0 \cdot 10^{-A} \tag{2.17}$$

$$I_a(t) = I_0\,(1 - 10^{-A_t}) \tag{2.18}$$

Actinometry is generally performed by creating a solution of an actinometer that has been well-characterized and its quantum yield is known. The actinometer is placed in a cuvette and irradiated under the same conditions as the systems of interest for an exact time period. By definition, the infinitesimal change in the number of actinometer molecules due to absorbed

photons per infinitesimal time change is equal to the quantum yield of the photochemical reaction times the number of photons absorbed per infinitesimal time change, and is written mathematically here

$$-\frac{dN_{actinometer}}{dt} = \frac{\Phi_{rxn} \cdot N_{photons,abs}}{dt} \tag{2.19}$$

Assuming the cuvette is rectangular, it has a volume V = $a \cdot l$ where a is the surface area of the cuvette and l is its width or path length. Dividing the equation above by the volume and Avogadro's number results in the following equation

$$-\frac{d[actinometer]}{dt} = \frac{\Phi_{rxn} \cdot mol_{photons,abs}}{dt \cdot a \cdot l} \tag{2.20}$$

But the number of photons absorbed divided by the area and time is equivalent to the photon flux absorbed, I_a, from above. Therefore the following equation can be written

$$-\frac{d[actinometer]}{dt} = \frac{\Phi_{rxn} \cdot I_a}{l} \tag{2.21}$$

Now multiply both sides of the previous equation by ε_{act} and l and then use the relationship that A = ε l c and the following equation appears

$$-\frac{d[actinometer]}{dt} \cdot \varepsilon_{act} \cdot l = -\frac{dA_{act}}{dt} = \varepsilon_{act} \cdot \Phi_{rxn} \cdot I_a \tag{2.22}$$

Finally, replacing the term I_a with the definition from above reveals the following differential equations

$$\frac{dA_{act}}{dt} = -\varepsilon_{act} \cdot \Phi_{rxn} \cdot I_0 \cdot (1 - 10^{-A_{act}}) \tag{2.23}$$

$$\frac{dA_{act}}{1 - 10^{-A_{act}}} = -\varepsilon_{act} \cdot \Phi_{rxn} \cdot I_0 \cdot dt \tag{2.24}$$

After a long integration from A_0 to A_t (corresponding to t = 0 to time t) that is not shown because there is no chemistry involved (only mathematics), the following equation falls out for I_0, the photon flux

$$I_0 = \frac{1}{\varepsilon_{act} \cdot \Phi_{rxn} \cdot \Delta t \cdot \ln 10} \ln\left(\frac{e^{A_0 \ln 10} - 1}{e^{A_t \ln 10} - 1}\right) \quad (2.25)$$

The units of I_0 from the equation above are $\frac{mol\ cm}{L\ time}$ which is similar to the original definition. By converting 1 L into 1000 cm^3, (i.e. dividing I_0 by 1000), the units become $\frac{mol}{cm^2\ time}$, which is identical to the dimensions given in the original definition.

$$I_0 = \frac{1}{\varepsilon_{act} \cdot \Phi_{rxn} \cdot \Delta t \cdot \ln 10 \cdot 1000} \ln\left(\frac{e^{A_0 \ln 10} - 1}{e^{A_t \ln 10} - 1}\right) \quad (2.26)$$

With the derivation and conversion to the proper units complete, it is now possible to use the method of actinometry, which is described in detail in Chapter 3, to find the photon flux of the irradiation source. This value of I_0 will be used to find the number of photons absorbed in the kinetics experiments of the thymine model systems which will then allow for the calculation of the quantum yields of photodegradation.

Chapter 3
Experimental Methods

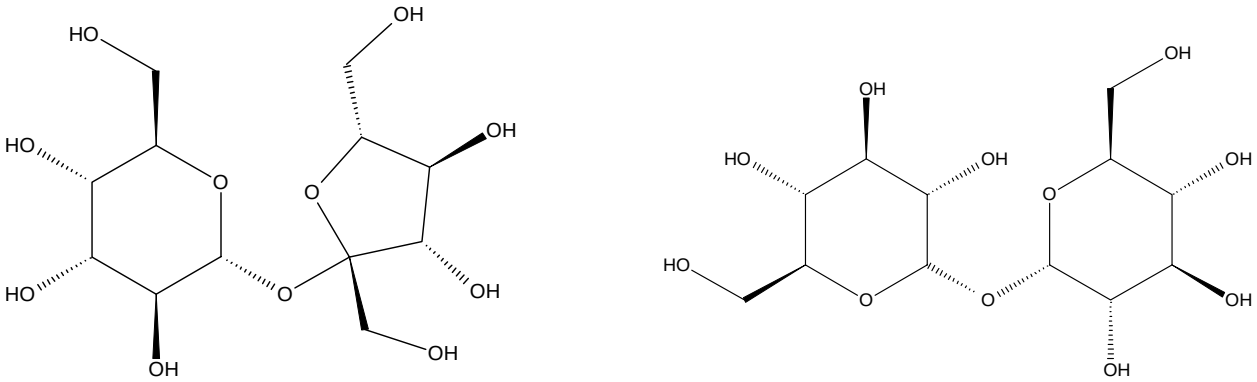

a) b)

Figure 3.1: Structures of the sugars used for encapsulation: a) sucrose, b) trehalose

The most important part of this experiment was the development of a room temperature sugar glass to encapsulate various DNA model systems for irradiation experiments. For this study sucrose (β-D-fructofuranosyl-(2→1)-α-D-glucopyranoside) and trehalose (α-D-glucopyranosyl α-D-glucopyranoside) were used because they have previously been shown to encapsulate the protein tryptophan for structural studies.[25,26] Figure 3.1 above shows the structures of sucrose and trehalose used in the experiments, which were obtained from Sigma-Aldrich chemical company with a purity ≥ 99%. The solvent used to dissolve the sugars and DNA model systems was 50 mM phosphate buffer at pH 7 instead of nanopure water. Samples of thymine bases and TMP were also obtained from Sigma-Aldrich chemical company with a

purity ≥ 99%. Samples of dTpdT were custom made from Midland Certified Reagent Company with a purity ≥ 99%. Absorbance measurements were done using a Perkin Elmer Lambda 25 UV-Vis spectrophotometer. CD measurements were made using an AVIV Model 202 Circular Dichroism spectrophotometer.

3.1 Encapsulation of Thymine Systems

The quintessential aspect of this study is to examine how structural changes in thymine systems affect the rate of photodimerization. In order to do this, a room temperature sugar glass was used to encapsulate the various thymine systems (free thymine, TMP, and dTpdT). However, the sugar glass had to have several properties to be used successfully in irradiation and CD experiments. The particular region of the UV-Visible spectrum of interest ranges from 400-200 nm, which falls mostly in the UVC spectrum. Therefore, it was imperative that the sugar glass did not absorb in this range.

Solutions of the thymine systems were created by dissolving free thymine, TMP, and dTpdT in a 50 mM phosphate buffer at pH 7 until the absorbance at 267 nm was between 0.5 and 1.0. The room temperature glass was created by dissolving 300 mg of sucrose and 300 mg of in 500 μL of nanopure water. To encapsulate the thymine systems in the glass, 400 μL of the buffered solution containing thymine, TMP, or dTpdT was mixed with 100 μL of the sucrose/trehalose sugar solution. Blank glasses were made by mixing 400 μL of buffer with 100 μL of the sugar precursor. The resulting solution was placed on a quartz window for kinetics experiments or a 1 mm quartz cuvette for CD experiments and allowed to dry overnight. After drying at room temperature, a solid, sticky glass was formed. A UV-Visible absorption spectrum was taken after drying to determine if the thymine systems were successfully

encapsulated. If the absorbance peak at 267 nm retained an OD range of 0.5 – 1.0, the sample was considered to be successfully made and was used for either CD or kinetics experiments.

3.2 CD Experiments

To collect CD data 1 mm quartz cuvettes were either filled with solution or coated with sugar glass. For all CD data, the following system specifications were always used: a wavelength range of 320-190 nm with a bandwidth of 2.00 nm, a collection speed of 1 nm per second averaged over 5 scans, and a constant temperature of 25.00 ± 0.01 °C. The solution phase experiments consisted of two parts. In the first part CD spectra were collected for buffered solutions of free thymine, TMP, and dTpdT. For the second part, 400 μL of the buffered thymine systems was mixed with 100 μL of the sugar glass precursor and placed inside a 1 mm cuvette. The CD spectra were then collected for the combined buffer and sugar precursor solution to examine any effects the sugars had on the various thymine systems. The CD spectrum of the solvent and of the solvent and sugar combination was taken to correct for the background signal of these species. For the sugar glass experiments, the 1 mm cuvettes coated with the sugar glass encapsulation were used as the samples. The CD data for a 1 mm cuvette coated with sugar glass encapsulating only phosphate buffer was used to correct for the background signal of the dried glass.

3.3 Irradiation Experiments

The kinetics of the thymine systems in solution and in glass were studied by irradiating samples and monitoring changes in absorbance. In order to calibrate the photon flux of the irradiation source, it was imperative to perform actinometry. The photon flux then made it possible to calculate the quantum yields of the thymine species and gain a quantitative understanding of the rates of photodimerization in different environments.

3.3.1 Actinometry

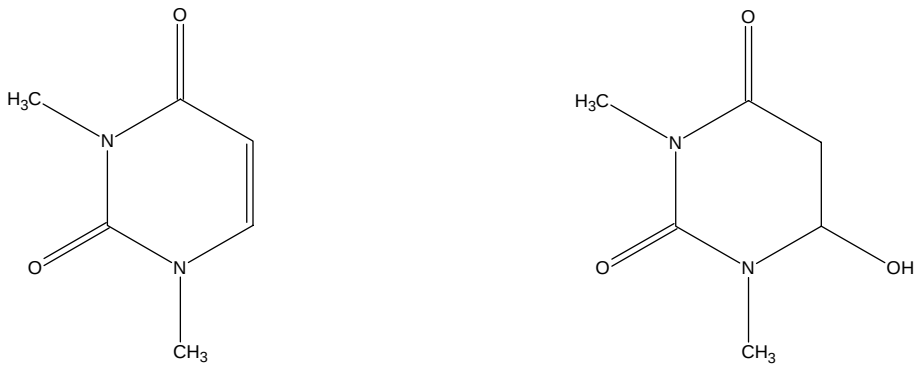

a) b)

Figure 3.2: Structure of the molecule used for actinometry and its photohydrate; a) 1,3-dimethyluracil, b) 1,3-dimethyl-6-oxy-hydrouracil

Perhaps the most important aspect of the kinetics experiments was the calibration of the photon flux from the lamp used to irradiate the thymine samples. A rigorous discussion of the mathematics behind the actinometry was given in the previous chapter. The molecule used to perform the actinometry was 1,3-dimethyluracil (DMU) which, when irradiated with the same light source as the kinetics experiments, reacts with water to form the photohydrate, 1,3-dimethyl-6-oxy-hydrouracil. Both of these molecules are shown above in Figure 3.2. The first step of actinometry was to prepare a sample of DMU which was done by dissolving it in 50

mM phosphate buffer at pH 7 until the absorbance was between 0.5 and 1.0 at 254 nm in a 1 mm quartz cuvette. A 254 nm germicidal lamp was placed inside a Rayonet Photochemical Reactor and allowed to run for thirty minutes before any irradiation took place. After the germicidal lamp was sufficiently warmed up, the sample of DMU was placed in the exact location that the thymine samples would be placed inside reactor. The sample of DMU was irradiated for a precisely measured quantity of time, usually 10-15 minutes, before and after irradiation experiments, and a second absorption spectrum was collected. The initial absorbance and absorbance after irradiation of DMU were recorded, and using the results from Chapter 2 the average photon flux was calculated.

3.3.2 Kinetics Experiments

The rates of photodimerization of free thymine, TMP, and dTpdT, which are shown on the next page in Figure 3.3, were studied in phosphate buffer with and without sugar glass precursor being added and encapsulated in the sugar glass. Buffered solutions of the thymine systems were made by dissolving solid samples into phosphate buffer until the absorbance was between 0.5 and 1.0. The combined buffer and sugar solutions were created by making the sugar glass precursor as discussed above and placing it directly into a 1 mm cuvette without allowing it to dry. Sugar glass encapsulations were also prepared using the method from above. Prepared samples were placed in the photoreactor and irradiated with a 254 nm germicidal at the same location the DMU samples were for the actinometry. Irradiation was interrupted on regular time intervals to collect UV-Vis spectra. Irradiation experiments typically lasted 50 minutes with UV-Vis spectra being collected every thirty seconds for the first 5 minutes, every minute for the

next 5 minutes, then every 5 minutes until photodegradation was complete and the system was in equilibrium. This marked the completion of the experiment.

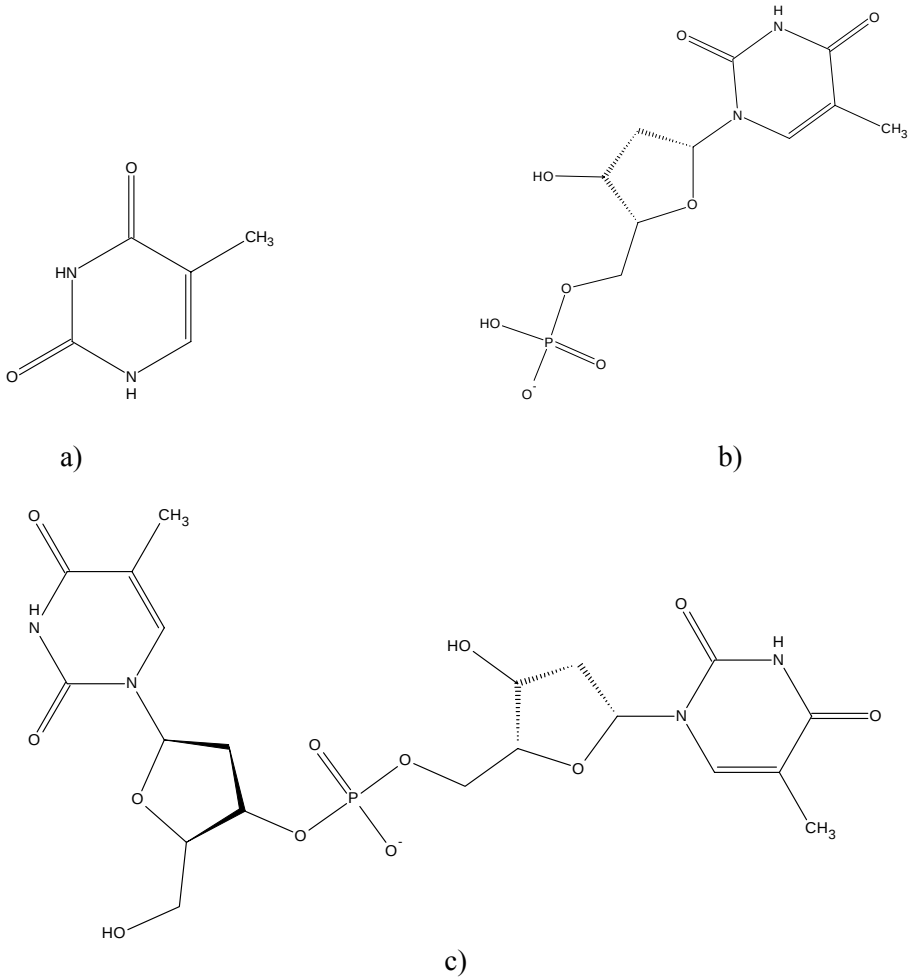

Figure 3.3: Structures of the thymine model systems; a) thymine, b) thymidine monophosphate (TMP), c) thymidyl-3'→5'-thymidine (dTpdT)

Chapter 4
Results and Analysis

4.1 Kinetics Experiments

The first set of experiments performed was to probe the kinetics of free thymine, TMP, and dTpdT in phosphate buffer, phosphate buffer mixed with the sugar glass precursor, and in sugar glass. All samples were prepared as discussed above in Chapter 3 and actinometry was performed before and after all irradiation experiments. The first part of this section describes a set of experiments performed to test the validity of the first principles derivation followed by a discussion of the results. The second part of section 4.1 describes the results of the kinetics experiments done on the thymine systems also followed by a discussion.

4.1.1 Validation of an Actinometrical Derivation

A test on the derivation for calculating the photon flux using actinometry was performed as outlined in Chapter 3 but using DMU in buffer for a kinetics experiment instead of a thymine molecule. The objective was to calculate the photon flux of the light source in the photoreactor as it was done for all of the thymine system kinetics and then calculate the quantum yield for DMU. If there is a serious issue with the mathematical treatment of the actinometry experiments, then it would be unlikely that the calculated quantum yield of photohydration for DMU would match literature values.

A sample of DMU was placed in the precise location that all future samples would be placed and irradiated for 10 minutes. A second absorption spectrum was collected to find the final absorbance at 254 nm after irradiation. This was repeated two more times before the kinetics experiments on DMU were done and then three times afterwards. The photon flux (I_0 with units $\frac{mol}{cm^2 min}$) was calculated for each trial and then averaged. The results are shown in Table 4.1 below, where Trials 1-3 represent measurements before the experiment and 4-6 represent measurements afterwards.

Trial Number	**Initial Absorbance at 254 nm**	**Final Absorbance at 254 nm**	**Photon Flux ($\cdot 10^{-7}$)**	**Average Photo Flux ($\cdot 10^{-7}$)**
1	1.0442	0.9522	1.249	
2	1.0419	0.9500	1.248	
3	1.0406	0.9480	1.251	1.2487 ± 0.0026
4	1.0440	0.9523	1.245	
5	1.0436	0.9518	1.247	
6	1.0418	0.9496	1.252	

Table 4.1: Results of actinometry experiments performed to find the photon flux.

A sample of DMU was diluted by about 10 % of the original concentration from the stock solution of DMU used for the actinometry. This sample was then placed directly into the same location as each of the samples was in the actinometry measurements. The DMU sample was then irradiated and interrupted at regular time intervals to collect UV-Vis spectra, which would be used to calculate the concentration of DMU after each time period of irradiation. Figure 4.1 on the next page shows the results of irradiating DMU over the course of 25 minutes. As a result of the photohydration reaction that occurs

when DMU is irradiated with 254 nm light, the absorbance decreases during the experiment. The absorbance at 254 nm was taken from the data and using Beer's Law, the concentration of DMU was calculated at each time interval. With the calculated value of I_0 from the actinometry done before and after the irradiation experiment, the number of photons absorbed by the DMU in the kinetics experiment

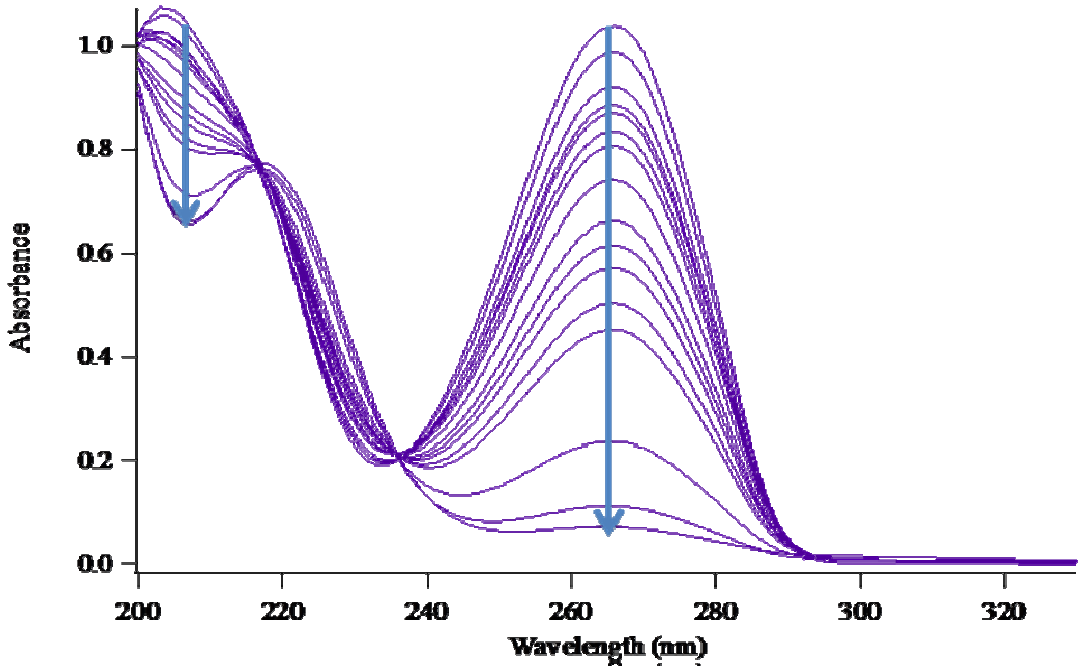

Figure 4.1: UV-Vis spectra at different time intervals of irradiation for DMU in phosphate buffer. The blue arrows have been added to show the decrease in absorbance during the irradiation process.

is calculated using a few of the results from Chapter 2 and multiplying by the time of irradiation and correcting for the path length of the cuvette. This is shown mathematically below

$$photons\ absorbed = \frac{I_a \cdot t}{l} \tag{4.1}$$

$$photons\ absorbed = \frac{I_0\ \left(1-e^{-A_t \cdot ln10}\right) \cdot t}{1000 \cdot l} \tag{4.2}$$

The units of photons absorbed are simply the units of I_0 ($\frac{mol}{cm^2\ min}$) multiplied by a time unit (minutes) and divided by the path length (cm). Therefore, the final units of photons absorbed by the conventions used in these experiments is $\frac{mol}{cm^3}$, which will be very important when discussing

the calculation of the quantum yield of photodegradation for the thymine systems. Figure 4.2 shows a plot of the concentration of DMU, which was calculated from the absorbance at 254 nm using $\varepsilon_{254} = 6300\ M^{-1}\ cm^{-1}$, versus the number of photons absorbed.

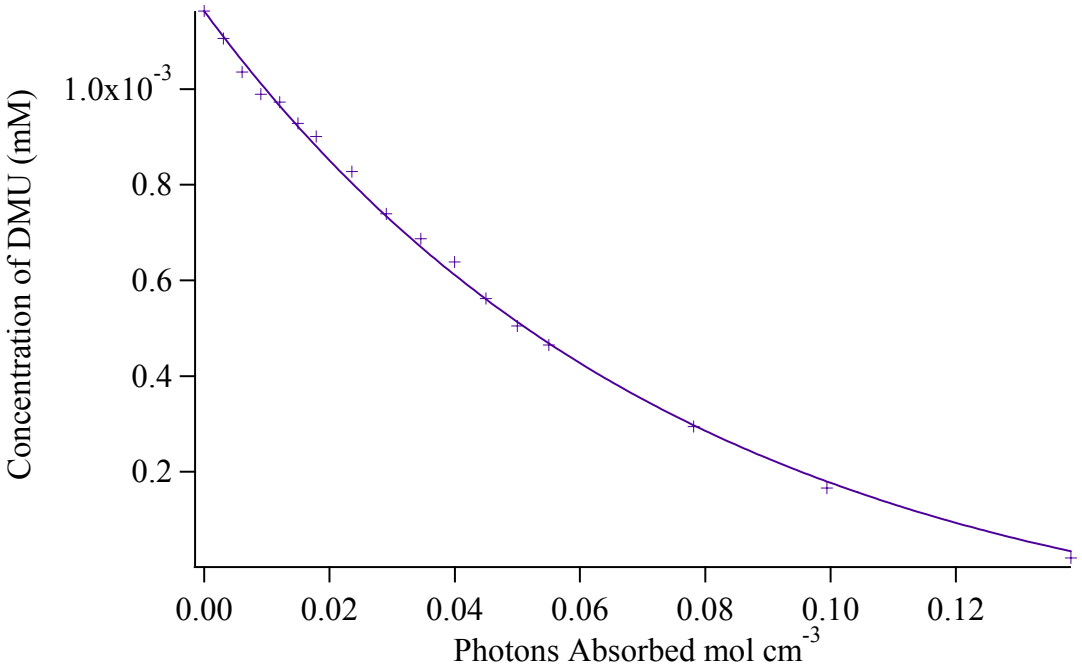

Figure 4.2: A plot of the concentration of DMU (in units of millimolarity) versus the number of photons absorbed by the DMU molecules.

The plot of points was fit to an exponential function of the form shown below

$$[DMU]_t = [DMU]_0 + A \cdot e^{-photons\ absorbed \cdot \tau} \tag{4.3}$$

The terms $[DMU]_t$ and $[DMU]_0$ represent the concentration after irradiation for time *t* and the initial concentration, respectively. The coefficient of the exponential is just a constant used for fitting purposes and τ represents another fitting constant. The quantum yield of hydration, Φ_{hyd}, for DMU was calculated using the method of initial slopes.[27,28] To calculate the quantum yield with this approach, the parameters from the exponential fit were plugged into Equation 4.3. The derivative of this function was then taken and evaluated at photons absorbed = 0, which gives the equation shown on the next page.

$$\Phi_{hyd} = |A \cdot \tau| \tag{4.4}$$

The reasoning behind this method of calculating the quantum yield is discussed in the above references and will be explored deeper in section 4.1.3 where it is more appropriate to discuss and more easily illustrated. A total of three kinetics experiments were performed with DMU and the parameter fits of each experiment, the corresponding quantum yield of photohydration, and an average quantum yield are shown below in Table 4.2.

Trial	A ($\cdot 10^{-3}$)	T	Φ_{hyd}	Average Φ_{hyd}
1	1.34 ± 0.15	9.91 ± 0.08	0.0133 ± 0.0013	
2	1.30 ± 0.03	10.01 ± 0.10	0.0130 ± 0.0015	0.0132 ± 0.0011
3	1.29 ± 0.07	10.12 ± 0.09	0.0131 ± 0.0007	

Table 4.2: The parameters and their uncertainties from fitting the data of a concentration versus photon absorbed plot for three trials. The quantum yield of hydration was found by using Equation 4.4.

As can be seen from above, the average quantum yield of hydration from the three trials was found to be 0.0132 ± 0.0011, which agrees with the literature value[29,30] of 0.0130 very closely. This suggests that the method chosen for calculating the photon flux from a first principles derivation and a quantum yield using the method of initial slopes is able to produce accurate results that agree with the literature. These two methods of analysis will be used to analyze the reaction kinetics for the thymine systems.

4.1.2 Results of Thymine System Kinetics Experiments

The next step that had to be taken after actinometry and before the kinetics experiments was to ensure that the samples were prepared properly and were ready for irradiation. Figure 4.3 on the next page shows the spectra of free thymine, TMP, and dTpdT in buffer, buffer mixed with the sugar glass precursor, and in the sugar glass. The spectra were also used for concentration corrections for both the kinetics and CD experiments by relating the initial absorbance to the initial concentration through Beer's Law. It is important to note that the concentration of each thymine system in buffer was higher than in buffer mixed with sugar solution and in the sugar glass. The mixed buffer and sugar solution had the lowest concentration because it was the most diluted. As the sugar glass formed, water was lost to the atmosphere and the concentration was partially restored, but because some water remained within in the sugar glass, the concentration did not obtain the value it was originally in buffer. Figures 4.4, 4.5, and 4.6 shown on the next three pages show the loss in absorbance versus wavelength as a function of irradiation time for each thymine system in buffer, buffer and sugar solution, and in the sugar glass, respectively.

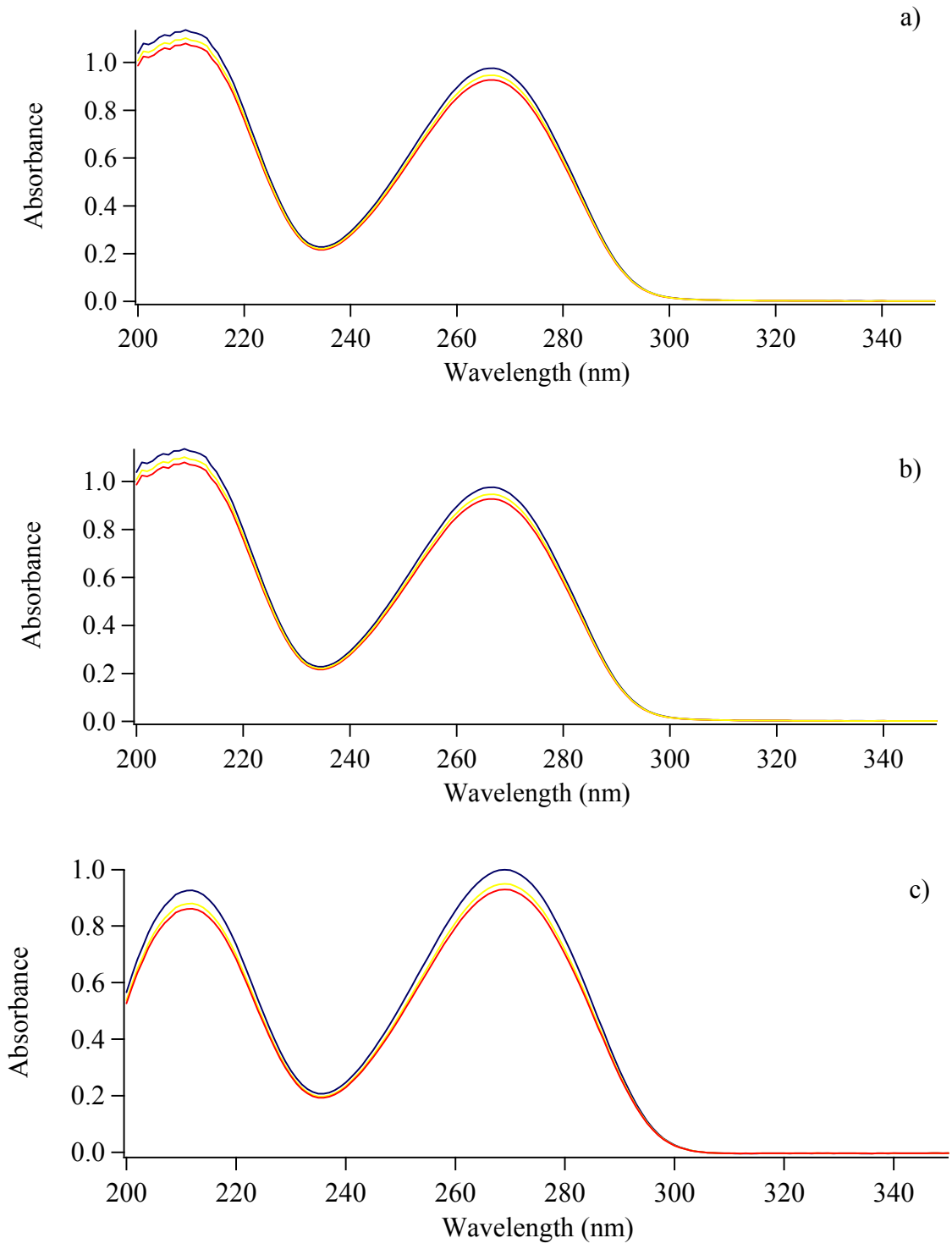

Figure 4.3: UV-Vis absorption spectra for a) thymine, b) TMP, and c) dTpdT in buffer (blue), buffer mixed with sugar solution (red), and in sugar glass (yellow).

4.1.3 Analysis and Discussion of Irradiation Experiments

Before beginning an analysis of the data, it is appropriate to model the kinetics of the thymine systems and discuss the reasoning behind using the method of initial slopes. As was pointed out in Chapter 1, the two main photoproducts that occur when two thymine bases photoreact are the cyclobutane pyrimidine dimer (CPD) and pyrimidine-(6-4)-pyrimidone photoadduct. The CPD, shown as T<>T, can be photoreversed with the same type of photon used to create it, but the photoadduct product cannot. The two reactions are coupled and their equations are shown below

$$T + T \leftrightarrow T <> T \tag{4.5}$$

$$T + T \rightarrow T(6-4)T \tag{4.6}$$

The change in the number of thymine molecule pairs (TT) is defined using the basic principles of kinetics and is given in Equation 4.7 (shown three pages from here).

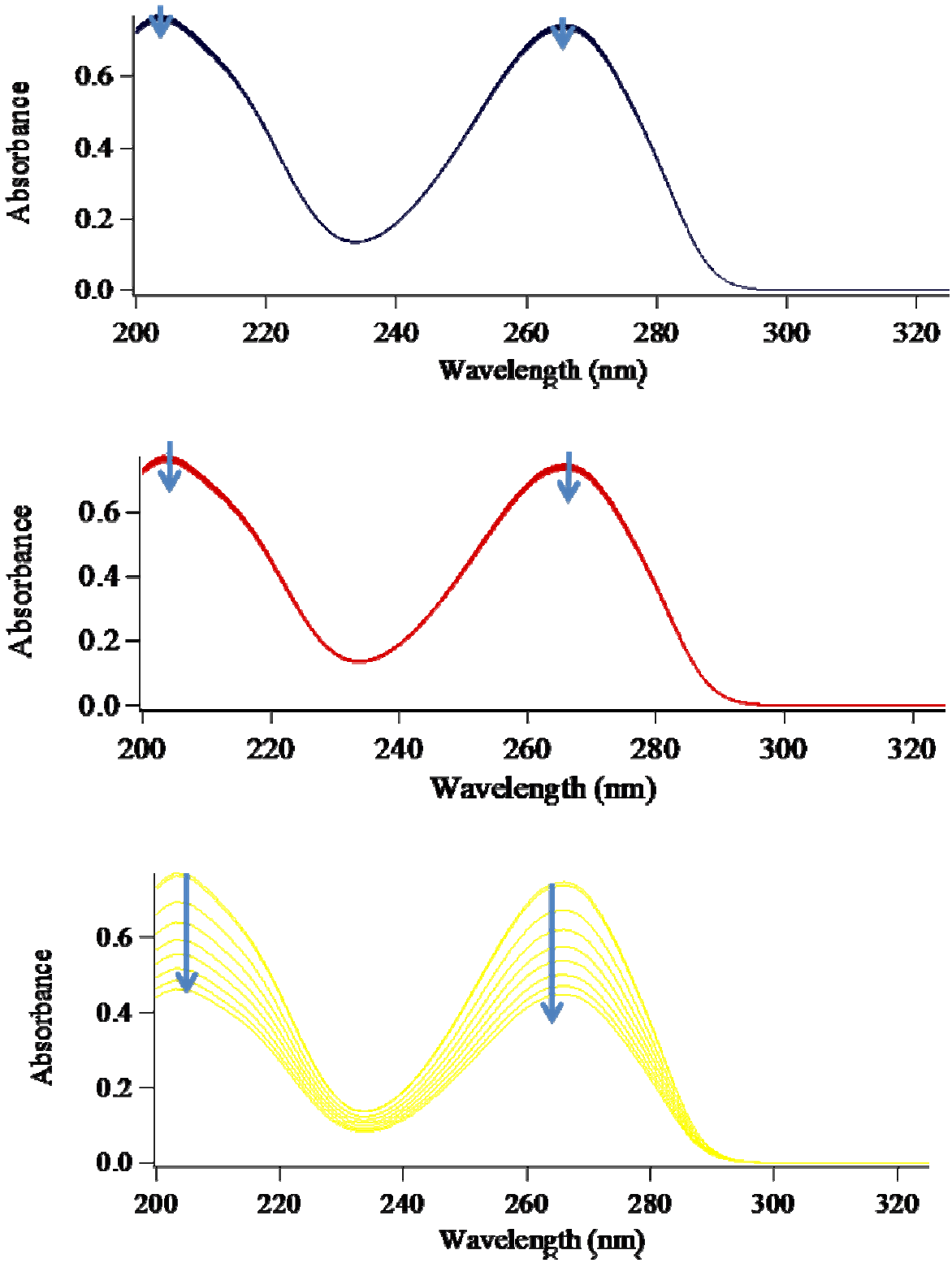

Figure 4.4: UV-Vis spectra at different time intervals of irradiation of thymine in buffer (blue), buffer and sugar solution (red) and in the sugar glass (yellow). The blue arrows have been added to show the decrease in absorbance during the irradiation process.

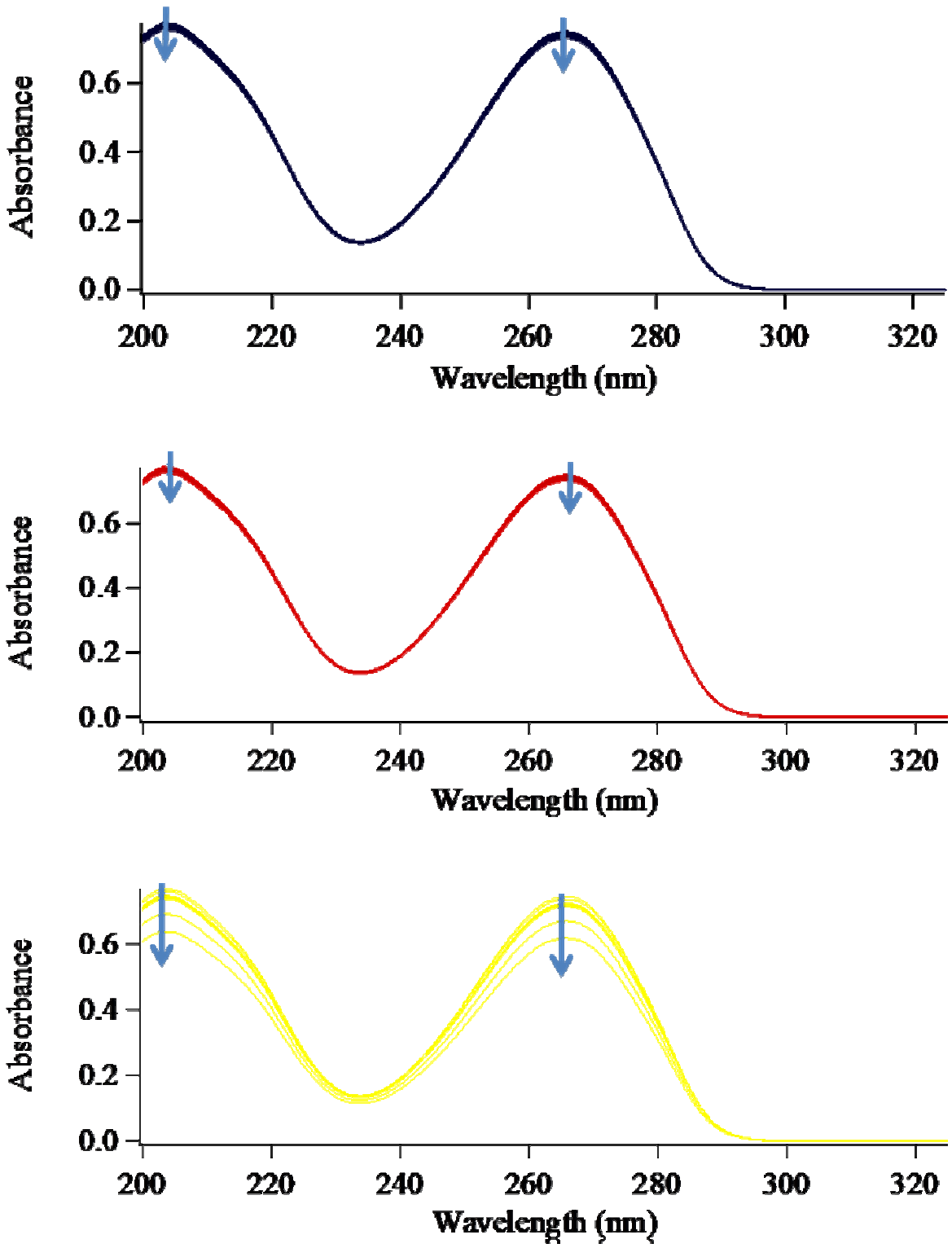

Figure 4.5: UV-Vis spectra at different time intervals of irradiation of TMP in buffer (blue), buffer and sugar solution (red) and in the sugar glass (yellow). The blue arrows have been added to show the decrease in absorbance during the irradiation process.

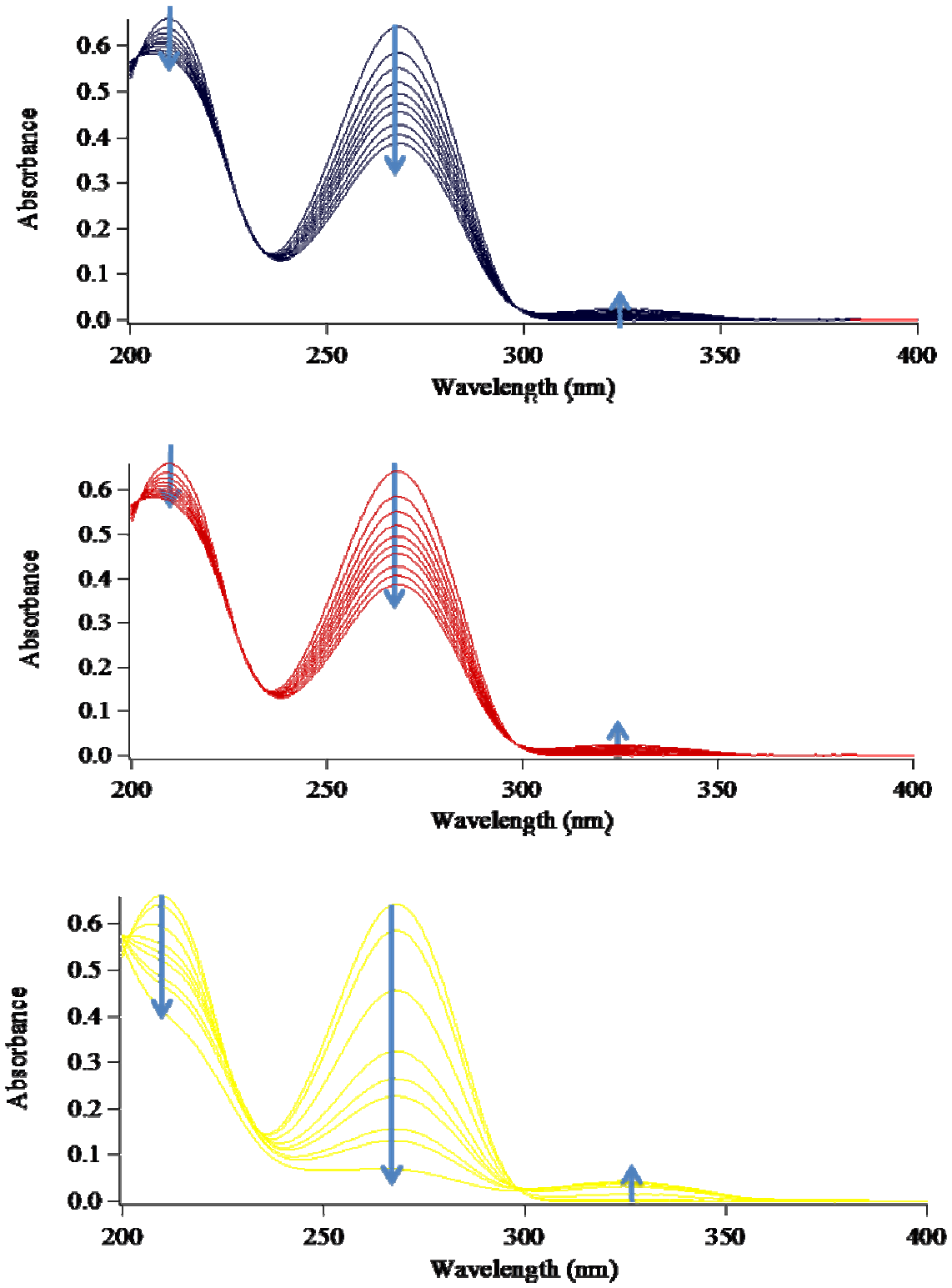

Figure 4.6: UV-Vis spectra at different time intervals of irradiation of dTpdT in buffer (blue), buffer and sugar solution (red) and in the sugar glass (yellow). The blue arrows have been added to show the decrease in absorbance during the irradiation process.

$$\Delta(number\ of\ TT\ molecues) = -\Phi_{dim} \cdot (photons\ absorbed\ by\ TT) - \Phi_{6-4} \cdot (photons\ absorbed\ by\ TT) + \Phi_{rev} \cdot (photons\ absorbed\ by\ CPD)$$

(4.7)

After collecting terms and defining the sum of the quantum yield of dimerization and 6-4 photoproduct formation to be the quantum yield of photodegradation, Equation 4.7 becomes

$$\Delta(number\ of\ TT\ molecues) = -\Phi_{photodeg} \cdot (photons\ absorbed\ by\ TT) + \Phi_{rev} \cdot (photons\ absorbed\ by\ CPD)$$

(4.8)

Dividing through by Avogadro's number and the volume (defined similarly in Chapter 2 as V = a · *l*, where *a* is the surface area of the cuvette and *l* is the path length), the rate equation becomes

$$\Delta[TT] = \Phi_{photodeg} \cdot \frac{mol_{photons,TT}}{a \cdot l} + \Phi_{rev} \cdot \frac{mol_{photons,CPD}}{a \cdot l} \quad (4.9)$$

Dividing Equation 4.9 by the increment of time that it is irradiated (Δt), and using the definition for the intensity of light using Equation 2.15, it can be shown that

$$\frac{\Delta[TT]}{\Delta t} = -\Phi_{photodeg} \cdot \frac{I_{a,TT}}{l} + \Phi_{rev} \cdot \frac{I_{a,CPD}}{l} \quad (4.10)$$

Appealing to Beer's Law once again, it can be shown that the ratio of intensity of photons absorbed by species X to the total intensity of light absorbed is equal to the ratio of the absorbance of species X divided by the total amount of absorbance, assuming there are no interactions between species X and anything else in the sample. Thus

$$\frac{I_{a,X}}{I_a} = \frac{A_X}{A} \quad (4.11)$$

Using Equation 4.11, Equation 4.10 becomes

$$\frac{\Delta[TT]}{\Delta t} = -\frac{\Phi_{photodeg}}{l} \cdot \frac{A_{TT}}{A} \cdot I_a + \frac{\Phi_{rev}}{l} \cdot \frac{A_{CPD}}{A} \cdot I_a \quad (4.12)$$

The total absorbance for this system is the sum of A_{TT} and A_{CPD}, which is shown in Equation 4.13 using Beer's Law

$$A_{TT} + A_{CPD} = A_{total} = l\,(\varepsilon_{TT} \cdot [TT] + \varepsilon_{CPD} \cdot [CPD]) \tag{4.13}$$

The ratio of A_{TT} and A_{CPD} to A_{total} is shown below in Equations 4.14 and 4.15

$$\frac{A_{TT}}{A_{total}} = \frac{\varepsilon_{TT}\cdot[TT]}{(\varepsilon_{TT}*[TT] + \varepsilon_{CPD}\cdot[CPD])} \tag{4.14}$$

$$\frac{A_{CPD}}{A_{total}} = \frac{\varepsilon_{CPD}\cdot[CPD]}{(\varepsilon_{TT}\cdot[TT] + \varepsilon_{CPD}\cdot[CPD])} \tag{4.15}$$

Utilizing Equations 4.14 and 4.15 along with the definition of I_a from Equation 2.17 and taking the limit as Δt goes to zero, Equation 4.12 becomes

$$\frac{d[TT]}{dt} = \frac{I_0\left(1-e^{-A\ln 10}\right)}{l}\left(-\Phi_{photodeg}\,\frac{\varepsilon_{TT}\cdot[TT]}{(\varepsilon_{TT}\cdot[TT] + \varepsilon_{CPD}\cdot[CPD])} + \Phi_{rev}\,\frac{\varepsilon_{CPD}\cdot[CPD]}{(\varepsilon_{TT}\cdot[TT] + \varepsilon_{CPD}\cdot[CPD])}\right) \tag{4.16}$$

In order to make an attempt at integrating this, all the variables should be made into [TT]. This can be accomplished by using conservation of mass: $[TT]_0 = [TT]_t + [CPD]_t + [6-4]_t$

As will be seen from the data soon, the formation of photoadduct is incredibly small in thymine and TMP and therefore it will be neglected in the rest of the derivation. However, in dTpdT there is a significant amount of photoadduct that forms and this assumption cannot be made. Even with the assumption, the derivation still fails to produce a useful result, so leaving the photoadduct concentration in the equation for the dTpdT kinetics does not matter because it will be an even more complicated integral to solve. Plugging the mass balance into 4.16 and assuming no photoadduct product gives the following Equation 4.17

$$\frac{d[TT]}{dt} = \frac{I_0\left(1-e^{-A\ln 10}\right)}{l}\left(-\Phi_{photodeg}\,\frac{\varepsilon_{TT}\cdot[TT]}{\left(\varepsilon_{TT}\cdot[TT] + \varepsilon_{CPD}\cdot([TT]_0 - [TT]_t)\right)}\right.$$
$$\left. + \Phi_{rev}\,\frac{\varepsilon_{CPD}\cdot([TT]_0 - [TT]_t)}{(\varepsilon_{TT}*[TT] + \varepsilon_{CPD}\cdot([TT]_0 - [TT]_t))}\right)$$

Upon integration of Equation 4.17, one finds that it is painfully difficult and is impossible to find an analytical solution without making further assumptions. The only assumption that came close to having an analytical solution was assuming that $\varepsilon_{TT} >> \varepsilon_{CPD}$, but that only led to a nasty Lambert Function of the form W(*f*). The issue with trying to integrate this Lambert Function is that it does not diverge across any of the approximations that were applicable to experimental conditions according to the literature.[31] The point of the derivation of the kinetics thus far was to show that it is very difficult, if not impossible, to get an analytical solution to the differential equation shown above. It was hoped that an analytical solution would allow the kinetics to be mapped out exactly, and then using experimental data the quantum yield of photodegradation and quantum yield of photoreversal could be calculated. Since this method has failed, the method of initial slopes was chosen.

In the method of initial slopes, the goal is to examine Equation 4.17 in the limit as time goes to zero which is the same limit as [CPD] goes to zero. In this limit, the rate expression becomes much simpler

$$\frac{d[TT]}{dt} = -\Phi_{photodeg}\frac{I_0(1-e^{-A\cdot\ln 10})}{l} \tag{4.18}$$

Based on previous experience with fitting other photochemical reaction kinetics (such as DMU) and working with thymine systems for so long, the kinetics were heuristically fit to a function of the form shown below, where k is a fitting factor with units of inverse time

$$[TT] = [TT]_0 + [TT]_{eq}\cdot e^{-k\cdot t} \tag{4.19}$$

When the derivative of this function is taken, the following result is obtained

$$\frac{d[TT]}{dt} = -[TT]_{eq}\cdot k\cdot e^{-k\cdot t} \tag{4.20}$$

At time $t = 0$, the derivative takes the value of $-k\,[TT]_{eq}$, which can be set equal to Equation 4.18 evaluated at time $t = 0$. This is shown below in Equation 4.21

$$\Phi_{photodeg}\frac{I_0(1-e^{-A_0\cdot\ln 10})}{l} = k\cdot[TT]_{eq} \tag{4.21}$$

Rearranging this equation to isolate $\Phi_{photodeg}$ gives

$$\Phi_{photodeg} = \frac{l\cdot k\cdot[TT]_{eq}}{I_0\,(1-e^{-A_0\cdot\ln 10})} \tag{4.22}$$

Quantum yields are meant to be unitless quantities that represent a ratio. Therefore, there should be no units on Equation 4.22, but upon examination there is an inconsistency: the units of the numerator are $\frac{cm\,M}{time} = \frac{cm\,mol}{time\,L}$ while the units of the denominator are $\frac{mol}{cm^2\,time}$. This can be reconciled by using the conversion factor that 1 L = 1000 cm^3, which changes Equation 4.22 into a useful equation for calculating the quantum yield of photodegradation

$$\Phi_{photodeg} = \frac{l\cdot k\cdot[TT]_{eq}}{I_0\,(1-e^{-A_0\cdot\ln 10})\,1000} \tag{4.23}$$

From here it is possible to calculate the quantum yield of photoreversal by noting that at equilibrium, [TT] = $[TT]_{eq}$ and that $\frac{d[TT]}{dt} = 0$. Since the main objective of this study was to examine the effects that different environments had on the kinetics of photodegradation and not photoreversal, this topic will not be explored any further and will be left as an exercise to the reader if he or she so desires.

With a thorough discussion of the background behind the analysis complete, the results are shown in Figure 4.7 on the next page. Figures 4.4, 4.5, and 4.6 from above show a decrease in absorbance at 260 nm indicating a loss of the thymine chromophore as the photoreaction takes place. For the dTpdT systems, there is a noticeable increase in absorbance at 325 nm indicating the formation of the (6-4)-photoadduct. The kinetics of each system will be studied by finding the concentration of each thymine species at 260 nm, using ε_{260} = 17200 M^{-1} cm^{-1}, and then plotting it against the number of photons absorbed calculated from the photon flux of the light source and Equation 4.2.

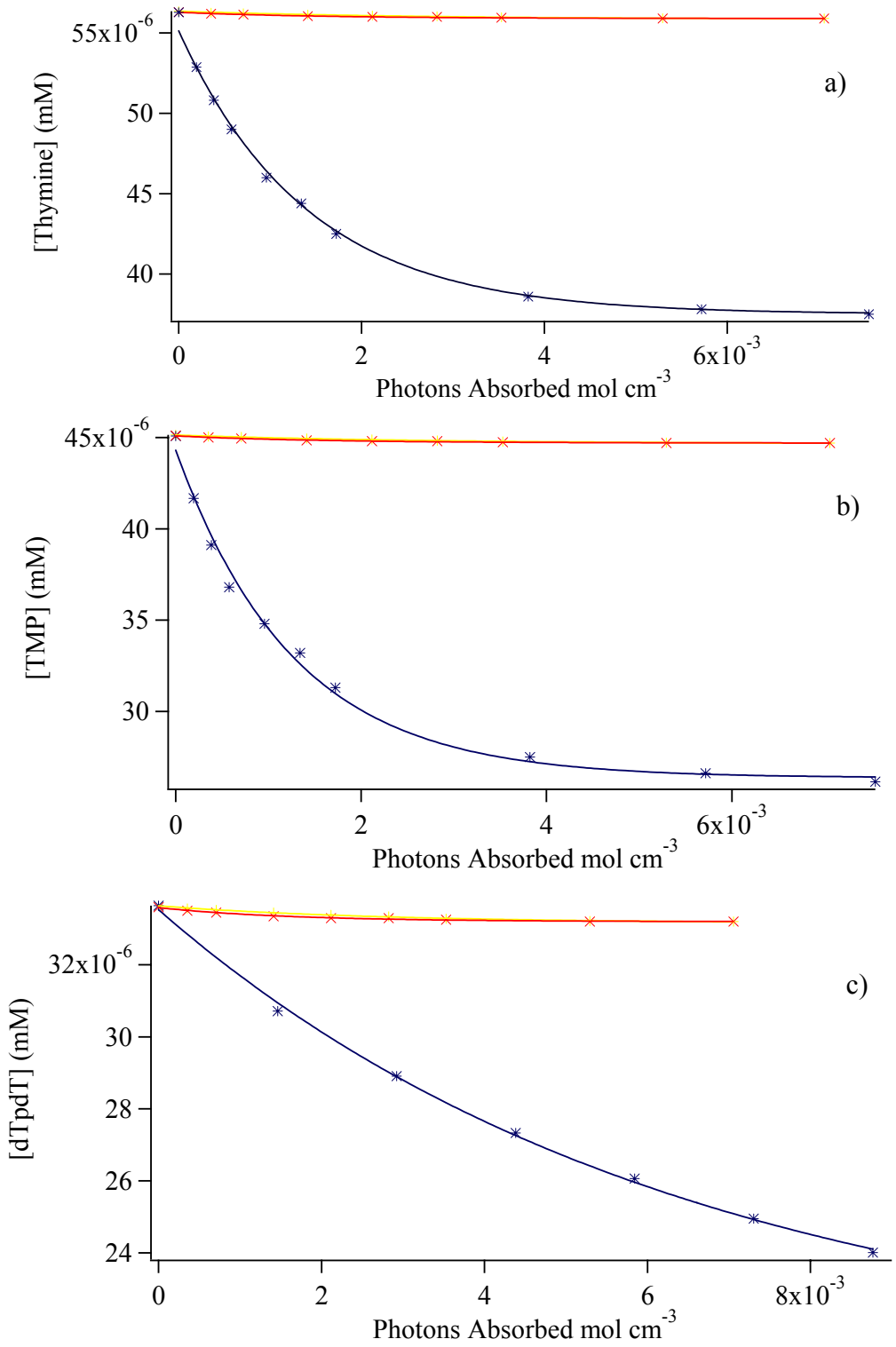

Figure 4.7: Kinetics plots for a) free thymine bases, b) TMP, and c) dTpdT in buffer (yellow curve), buffer and sugar solution (red curve), and in sugar glass (blue curve).

The curves shown above in Figure 4.7 were all fit to exponential functions of the form

$$[TT]_{photons_{abs}} = [TT]_0 + [TT]_{eq} \cdot e^{-k \cdot photons_{Abs}} \tag{4.23}$$

Equation 4.23 is very similar to Equation 4.19, but the subtle difference is that it is not being fit as a function of time anymore, but rather as a function of the number of photons absorbed. Plugging Equation 4.2 into Equation 4.23 to replace the number of photons absorbed with the time of irradiation gives

$$[TT]_t = [TT]_0 + [TT]_{eq} \cdot e^{-k \frac{I_0 \left(1-e^{-A_t \cdot \ln 10}\right) \cdot t}{1000 \cdot l}} \tag{4.24}$$

The units of *k* in equation 4.24 have switched from being an inverse time dimension to inverse molarity dimensions. Using the method of initial slopes, the gradient of Equation 4.24 takes the form

$$\frac{d[TT]}{dt} = -k \cdot [TT]_{eq} \cdot \frac{I_0 \left(1-e^{-A_t \cdot \ln 10}\right)}{1000 \cdot l} \cdot e^{-k \frac{I_0 \left(1-e^{-A_t \cdot \ln 10}\right) \cdot t}{1000 \cdot l}} \tag{4.25}$$

Taking the time to be $t = 0$ and setting Equation 4.25 equal to 4.18 gives

$$k \cdot [TT]_{eq} \cdot \frac{I_0 \left(1-e^{-A_t \cdot \ln 10}\right)}{1000 \cdot l} = \Phi_{photodeg} \frac{I_0 \left(1-e^{-A_0 \cdot \ln 10}\right)}{l} \tag{4.26}$$

Cancelling like terms gives the formula used to calculate the quantum yield of photodegradation for each of the kinetics experiments from above

$$\Phi_{photodeg} = \frac{k \cdot [TT]_{eq}}{1000} \tag{4.27}$$

The factor of 1000 was already accounted for in the plots of Figure 4.7 when the concentration was made into millimolarity. If the plots were done in molarity versus photons absorbed, then the factor of 1000 would have to be applied to ensure the units match.

Table 4.3 on the next page shows the fitting factors k and $[TT]_{eq}$ for the plots in Figure 4.7 as well as the calculated quantum yields using Equation 4.27. Table 4.4 shows the averages of the quantum yields of all trials performed and compares them to literature values.[30]

System	Media	K	$[TT]_{eq}$ (mM)	$\Phi_{photodeg}$
Thymine	**Buffer**	0.385 ± 0.012	0.00130 ± 0.00010	0.050 %
Thymine	**Buffer + Sugar**	0.177 ± 0.006	0.00271 ± 0.00011	0.048 %
Thymine	**Sugar Glass**	2.74 ± 0.009	0.00215 ± 0.00017	0.591 %
TMP	**Buffer**	0.305 ± 0.009	0.000361 ± 0.000016	0.011 %
TMP	**Buffer + Sugar**	0.345 ± 0.008	0.000377 ± 0.000007	0.013 %
TMP	**Sugar Glass**	4.50 ± 0.13	0.000360 ± 0.000015	0.162 %
dTpdT	**Buffer**	0.725 ± 0.012	0.0255 ± 0.0009	1.85 %
dTpdT	**Buffer + Sugar**	0.779 ± 0.008	0.0246 ± 0.0012	1.92 %
dTpdT	**Sugar Glass**	0.856 ± 0.004	0.945 ± 0.006	80.9 %

Table 4.3: Parameter fits for each of the kinetics experiments shown in Figure 4.7. The quantum yield of photodegradation was calculated using Equation 4.27 and then converting into a percentage.

System	Literature Φ in Buffer	Φ in Buffer	Φ in Buffer + Sugar	Φ in Sugar Glass	$\frac{\Phi_{Sugar\ Glass}}{\Phi_{Buffer}}$
Thymine	0.047 ± 0.001 %	0.053 ± 0.010 %	0.051 ± 0.010 %	0.58 ± 0.03 %	11.37
TMP	0.010 ± 0.002 %	0.009 ± 0.001 %	0.015 ± 0.003 %	0.15 ± 0.07 %	16.67
dTpdT	2.0 ± 0.2 %	2.0 ± 0.4 %	2.1 ± 0.5 %	81.5 ± 1.9 %	40.75

Table 4.4: Comparison of the averaged experimental quantum yields over all trials with those from the literature. The ratio in the last column was done between experimental data, not literature.

As can be seen from Tables 4.3 and 4.4, the quantum yield of photodegradation in buffer for this study matches those of the literature very well. It is also important to note that the quantum yield

in buffer is very similar to that in the buffer and sugar solution, suggesting that the thymine systems are not photoreacting with the sucrose and trehalose sugars that make up the sugar glass. Finally, the quantum yield in the sugar glass is about 10-15 fold greater for free thymine bases and TMP, and over 40 fold greater for dTpdT. The hypothesis was that the sugar glass was creating an environment much more conducive to photodimerization by forcing a greater number of thymine molecules into the proper alignment. To investigate this further circular dichorism was used to examine the structural effects the sugar glass actually had on the thymine systems.

4.2 Circular Dichroism

4.2.1 Results of CD Experiments

After collecting the data on the CD instrument, the proper concentration corrections were made by finding the initial concentration and then using Equation 2.14 to find $\Delta\varepsilon$. Figure 4.8 on the next page shows the results of CD experiments for each thymine system in buffer, buffer and sugar solution, and in sugar glass. It is important to note that each spectrum was presented over the wavelength range of 220-320 nm because the ribose sugar of TMP and dTpdT absorbs around 190 nm.

4.2.2 Discussion of CD Results

The first plot in Figure 4.8 shows that there is no effect on the free thymine bases in any of three media over the examined wavelengths. A single thymine base is a planar, aromatic molecule with no chiral centers. Therefore, as expected, there is no CD signal observed. It is not clear from the CD spectra of thymine what, if anything at all, the sugar glass is doing to increase the rate of photodegradation. The second plot in Figure 4.8 shows a similar trend to that of free

thymine bases. Since TMP is a thymine molecule attached to a sugar which is attached to a phosphate group, many chiral centers are present in the molecule. Therefore TMP is CD active and a spectrum should be observed. The spectra for TMP in buffer, buffer and sugar solution, and sugar glass lie on top of each other very closely. This suggests that there is little to no conformational changes in the TMP structure. Again, it is not clear from the CD spectra why the TMP molecules have an increased rate of photodegradation in the sugar glass if its structure is not altered to a more conducive geometry for dimerization. The third plot in Figure 4.8 is the most interesting because it shows a deviation between the buffer spectrum and the sugar glass spectrum. The spectrum of the dTpdT encapsulated in the sugar glass is slightly red-shifted with the maximum of the peak occurring around 281 nm instead of being located at 276 nm as in the buffer and buffer and sugar solution. After examining the spectra of different DNA forms, which all exhibit different characteristics on a CD spectrum, it was found that the spectrum of B-form DNA with thymine bases present has a maximum CD signal around 281 nm.[32,33] This suggests that the thymine molecules in dTpdT are becoming more stacked as they would appear in B-form DNA. The increase in base stacking helps explain the increased rate of photodimerization for the dTpdT system.

Other work done on larger thymine systems such as the 18-mer of thymidylic acid, $(dT)_{18}$, show that varying the type of solvent affects the amount of base stacking.[34] The increased base stacking was observed by an increase in the CD signal for a particular wavelength, which was chosen to be 278 nm for $(dT)_{18}$.[34] In Figure 4.8 above, there is also an increase in CD signal at the slightly red-shift peak at 281 nm. This is further evidence in support of increased base stacking of the thymine molecules in dTpdT.

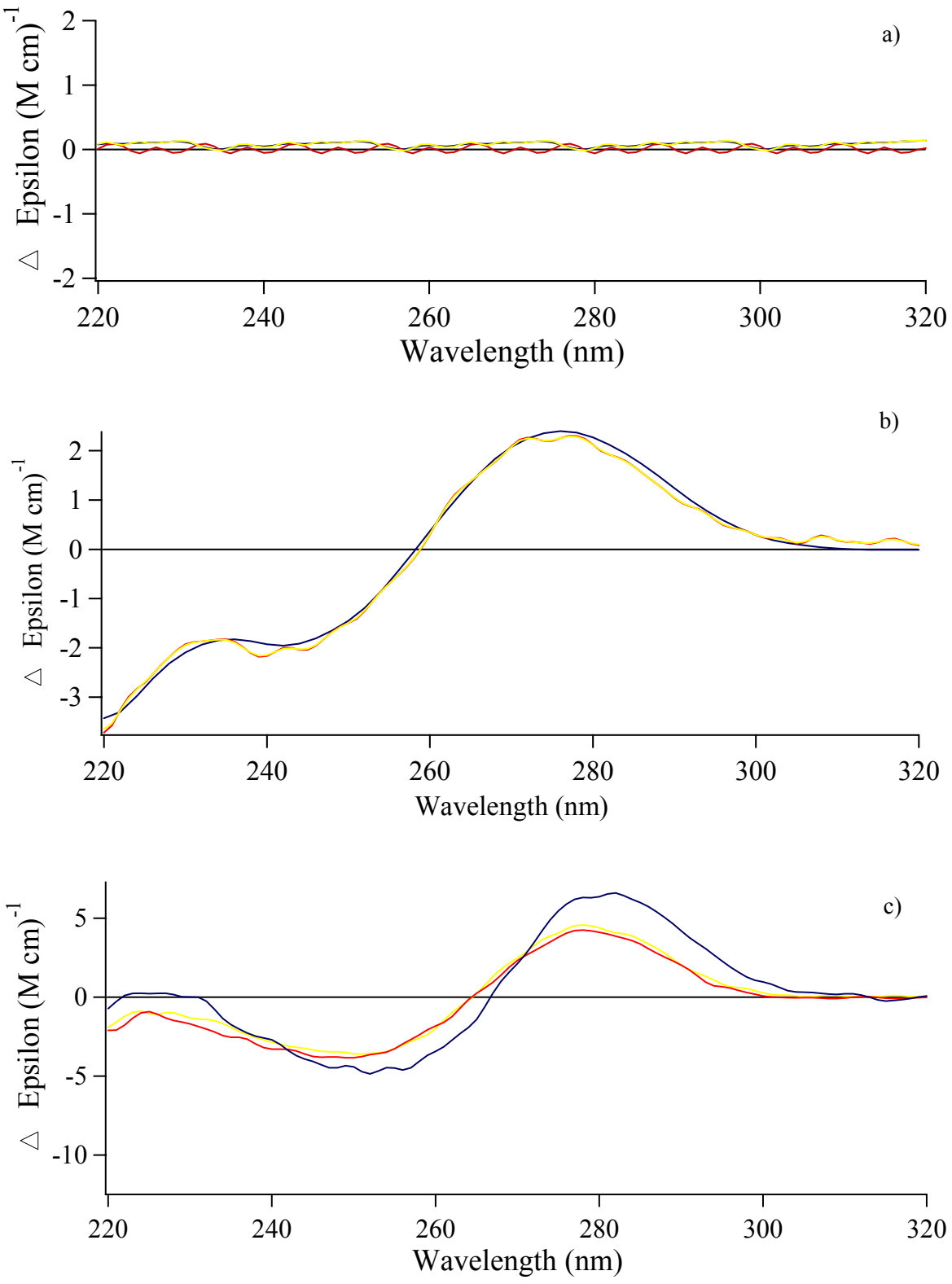

Figure 4.8: CD spectra of a) thymine, b) TMP, c) dTpdT in buffer (yellow curve), buffer and sugar solution (red curve), and sugar glass (blue curve).

Chapter 5
Conclusions

5.1 General Conclusions

From the results presented in Table 4.4, it is clear that the quantum yield of photodegradation is dramatically affected by the sugar glass. The quantum yield is very similar between the reactions performed in phosphate buffer and those performed in phosphate buffer mixed with the sugar glass precursor solution. This is strong evidence that supports the claim that thymine systems are not reacting with the sucrose or trehalose sugars present in the precursor solution and sugar glass. The question that needs to be answered now is why the quantum yields of photodegradation are increasing so much upon encapsulation in the sugar glass for each thymine system. The hypothesis made was that the sugar glass was either forcing or capturing a greater number of thymine bases into a geometry more conducive for photodimerization to occur. However, upon examination of the CD results, this could have only been possible for dTpdT because there were no observed conformational changes in free thymine bases or TMP. Therefore the increased rate of photodimerization must be a result of another factor: increased aggregation of thymine bases inside the sugar glass.

It has been shown that the rates of photodimerization of thymine monomers increases in frozen solutions and thin film alkaloids.[20,21] The reason for this is that an excited thymine monomer must diffuse in solution until it makes contact and properly align with another thymine base for dimerization to occur. Since it has been shown that thymine dimerization is an ultrafast process that occurs in less than one picosecond, photodimerization must occur via another path

than relaxation from an excited $^1\pi\pi^*$ state. Photodimerization of monomers must occur from longer lived excited triplet states that allow them more time to find a compatible partner. Relaxation from a singlet state is orders of magnitude faster than relaxation from a triplet state (see Chapter 1) because the former is an allowed transition (fluorescence), while the latter is a forbidden transition (phosphorescence). However, this effect was not observed in thymine multimers composed of two or more bases because photochemistry is more likely to occur between two intramolecular thymine bases than between two intermolecular ones. Therefore, the increased quantum yield of photodegradation for free thymine and TMP suggest that the sugar glass forms aggregates of thymine bases and TMP molecules. This increases the rate of photodimerization because excited thymine monomers do not have to travel as far to find another thymine base. Since an increase in the rate of dimerization between aggregated multimers was not observed in the literature, the increase in the quantum yield observed for dTpdT is largely a structural effect rather than a proximity effect. This is supported by a change in the conformation of dTpdT resulting in more B-form DNA characteristics such as increased base stacking. The results of this study support the ground state control theory that thymine dimerization is indeed structure dependent. However, there are still many more questions about the process of thymine dimerization that still need to be answered.

5.2 Future Work

The first set of experiments that would be useful in investigating the results of these experiments further would be to characterize the sucrose/trehalose glass. Since it is not quite clear how the sugar glass is actually affecting the thymine systems, using steady-state IR, Raman, and CD spectroscopy might provide clues about the structure of the sugar glass without any thymine

systems encapsulated in it. Spectra would be collected for sucrose and trehalose separately and compared with the spectra of sugar glass precursor solutions and hardened sugar glasses. By looking for characteristic marker bands on the IR, Raman, and CD spectra, it might become clear how the sugars are orienting themselves in solution versus in the sugar glass. It would also be interesting to pursue this study again with varying amounts of sucrose and trehalose used to make the sugar glass to see if the same effects on the quantum yield of photodegradation are observed. Also, varying the type of sugar would determine if the results are dependent on the chosen sugars used in these experiments or if this is a general result that would be observed for any type of sugar.

It would also be interesting to pursue experiments examining the encapsulated thymine systems on an ultrafast scale. Using a time-resolved UV-Vis transient absorption laser system, it would be possible to probe the lifetimes of the singlet and triplet states of the thymine systems in solution versus in sugar glass. As was discussed above, the main pathway that thymine monomers react is through the triplet state since it is longer lived and they require more time to find another thymine base. Therefore, the increased rate of dimerization in free thymine and TMP might be a result of aggregations of these molecules. This would lead to a decreased triplet lifetime because they are able to react faster and do not remain in this triplet state as long. Similar results might be observed for the singlet lifetime of dTpdT in the sugar glass because they may spend less time in the excited singlet state if the sugar glass is allowing for more dTpdT molecules to take on the proper conformation needed for dimerization.

References

1. Cadet, J., Vigny, P. *Bioorganic Photochemistry*, H. Morrison: Wiley, New York, 1990.
2. Taylor, J. S. *Acc. Chem. Res.* 1994, **27**: 76.
3. Vink, A. A., Roza, L. *J. Photochem. Photobiol. B Biol.* 2001, **65**: 101.
4. Melnikova, V. O., Ananthaswamy, H. N. *Mutat. Res.* 2005, **571**: 91.
5. Horton, H. R. et al. *Principles of Biochemistry*. Pearson Prentice Hall: Upper Saddle River, NJ, 2006.
6. Dahm, R. *Hum. Genet*. 2008, **122**: 565-81.
7. Freifelder, D. *The DNA Molecule: Structure and Properties: Original Papers, Analyses, and Problems*. W. H. Freeman and Company: San Francisco, 1978.
8. Kossel, A. *Arch. Anat. Physiol., Physiol. Abt*. 1891, **181**.
9. Levene, P. *J. Biol. Chem.* 1919, **40** (2): 415-24.
10. Astbury, W. *Symp. SOC. Exp. Bbl.* 1947. **1**: 66
11. Watson, J. D. and F. H. C. Crick. *Nature* 1953. **171**: 737-738.
12. Bloomfield, V. A., Crothers, D. M., and Ignacio Tinoco, Jr., *Nucleic Acids: Structures Properties, and Functions*. University Science Books: Sausalito, CA, 2000.
13. Middleton, C. T., et al. 2009. *Annu. Rev. Phys. Chem.* **60**: 217-39
14. Ghosh, A. and M. Bansai. *Acta Crystallogr D Biol. Crystallogr.* 2003. **59**: 620-626.
15. Basu, H., et al. 1988, *J Biomol Struct Dyn.* **6** (2): 299-309.
16. Schreier, W. J. et al. *Science*. 2007. **315** (5812): 625-629.
17. Hare, P. M., Crespo-Hernández, C. E., and B. Kohler. 2006. *J. Phys. Chem. B* **110**:18641–50.
18. Crespo-Hernández, C.E., Cohen, B., Hare, P. M. , and B. Kohler. 2004. *Chem. Rev.* **104**:1977–2019.
19. Law, Y. K., et al. *Biophys J.* 2008. **94** (9): 3590-3600.
20. Wang, S. Y., *Nature*. 1961. **190**: 690-694.
21. Smith, K. C., *Photochem. Photobiol.* 1963. **2**: 503-517.
22. Johnson Jr., C. W. Circular Dichroism Instrumentation. In *Circular Dichroism and the Conformational Analysis of Biomolecules; Fasman*, G. D., Ed.; Plenum Press: New York, 1996.
23. Skoog, D. A.; Holler, F. J.; Nieman, T. A. *Principles of Instrumental Analysis*; Thomson Learning, Inc.: United States, Fifth ed.; 2007.
24. Rodger, A.; B. Nordén. *Circular Dichroism & Linear Dichroism*. Oxford University Press: Oxford, New York, Tokyo; 1997.
25. Dashnau, J. L. et al. *Biophys. Chem*. 2005. **114**: 71-83.
26. Wright, W. W. et al. *Biophys. J.* 2003. **85**(3): 1980-1995.
27. Johns, H. E., *Photochem. Photobiol.* 1968. **8**: 547-563.
28. R.O. Rahn and H.G. Sellin. *Photochem. Photobiol.* 1979. **30:** 317–318.
29. H.J. Kuhn, S.E. Braslavsky and R. Schmidt. *Pure Appl. Chem.* 2004. **76:** 2105–2146.
30. T. Douki. *Photochem. Photobiol. Sci.* 2006. **5:** 1045–1051.

31. Chen, Y. Q. and K. L. Moore. *Automatica*. 2002. **38** (5): 891-895.
32. Johnson Jr., C. W. Determination of the conformation of nucleic acids by electronic CD. In *Circular Dichroism and the Conformation Analysis of Biomolecules*; Fasman, G. D., Ed.; Plenum Press: New York, 1996.
33. Baker, E. S. and M. T. Bowers. *J. Amer. Soci. Mass Spec.* 2007. **18** (7): 1188-1195.
34. Olmon, Eric. *Senior Honors Thesis*. Ohio State University: Columbus, Ohio, 2005.